Rice *SEPALLATA* genes *OsMADS5* and *OsMADS34* cooperate to limit inflorescence branching by repressing the *TERMINAL FLOWER1*-like gene *RCN4*

Wanwan Zhu[1] (iD), Liu Yang[1] (iD), Di Wu[1] (iD), Qingcai Meng[1], Xiao Deng[1], Guoqiang Huang[1] (iD), Jiao Zhang[1] (iD), Xiaofei Chen[1], Cristina Ferrándiz[2] (iD), Wanqi Liang[1] (iD), Ludovico Dreni[1,2] (iD) and Dabing Zhang[1,3] (iD)

[1]Joint International Research Laboratory of Metabolic and Developmental Sciences, State Key Laboratory of Hybrid Rice, Shanghai Jiao Tong University-University of Adelaide Joint Centre for Agriculture and Health, School of Life Sciences and Biotechnology, Shanghai Jiao Tong University, Shanghai, 200240, China; [2]Instituto de Biología Molecular y Celular de Plantas (IBMCP), Consejo Superior de Investigaciones Científicas-Universidad Politécnica de Valencia, Valencia, 46022, Spain; [3]School of Agriculture, Food and Wine, University of Adelaide, Waite Campus, Urrbrae, SA 5064, Australia

Authors for correspondence:
Dabing Zhang
Email: zhangdb@sjtu.edu.cn

Ludovico Dreni
Email: ludovico.dreni@gmail.com

Summary

- The spatiotemporal control of meristem identity is critical for determining inflorescence architecture, and thus yield, of cereal plants. However, the precise mechanisms underlying inflorescence and spikelet meristem determinacy in cereals are still largely unclear.
- We have generated loss-of-function and overexpression mutants of the paralogous *OsMADS5* and *OsMADS34* genes in rice (*Oryza sativa*), and analysed their panicle phenotypes. Using chromatin immunoprecipitation, electrophoretic mobility-shift and dual-luciferase assays, we have also identified *RICE CENTRORADIALIS 4* (*RCN4*), a *TFL1*-like gene, as a direct downstream target of both OsMADS proteins, and have analysed *RCN4* mutants.
- The *osmads5 osmads34* mutant lines had significantly enhanced panicle branching with increased secondary, and even tertiary and quaternary, branches, compared to wild-type (WT) and *osmads34* plants. The *osmads34* mutant phenotype could largely be rescued by also knocking out *RCN4*. Moreover, transgenic panicles overexpressing *RCN4* had significantly increased branching, and initiated development of c. 7× more spikelets than WT.
- Our results reveal a role for *OsMADS5* in panicle development, and show that *OsMADS5* and *OsMADS34* play similar functions in limiting branching and promoting the transition to spikelet meristem identity, in part by repressing *RCN4* expression. These findings provide new insights to better understand the molecular regulation of rice inflorescence architecture.

Introduction

The Poaceae, including many agriculturally important cereals such as rice (*Oryza sativa*), maize (*Zea mays*), barley (*Hordeum vulgare*), and wheat (*Triticum* spp.), produce a diverse range of complex inflorescence architectures, with distinct branched arrangements of flower-bearing spikelets that produce grain (Benlloch *et al.*, 2007; Kellogg, 2007). Rice, a grain crop that feeds more than half of the world's population, produces panicle-type compound racemes, normally with primary and secondary branches, which bear single-flowered spikelets.

Rice panicle architecture is defined by the sequential identity of the meristems produced by the shoot apical meristem (SAM) (Kyozuka *et al.*, 2014), and can be classified into developmental 'In' stages (Itoh *et al.*, 2005). Upon the initiation of reproductive development, the vegetative SAM is converted to inflorescence meristem (IM, stage In1), which is indeterminate and produces the main stem or rachis and several lateral primary branch meristems (PBMs) before it arrests (stages In2–In3). Each primary branch elongates and produces several lateral meristems (stages In4–In5); those formed near the rachis preferentially acquire the identity of secondary branch meristems (SBMs) and develop secondary branches, while the others directly become spikelet meristems (SMs). Finally, each PBM and SBM has a determinate fate and converts to a terminal SM (In6), and each SM produces the glumes and a floral meristem (FM), from which floral organ primordia differentiate (In7). At stage In8, floral organs develop and mature, while the rachis elongates rapidly. Key determinants of rice inflorescence architecture are thus the timing of IM arrest, the amount and proportion of SBMs/SMs, and the transformation of branch meristems into SMs. Early developmental events are often susceptible to abortion of branches and spikelet primordia, which can be triggered by physiological or environmental conditions to reduce the complexity and productivity of the mature panicle (Yamagishi *et al.*, 2004; Kato *et al.*, 2008).

To date, several key genes that determine meristem fate have been characterized in maize and rice, many of which encode transcription factors (TFs; Tanaka *et al.*, 2013; Zhang & Yuan, 2014). The SQUAMOSA promoter binding protein-like OsSPL14, also known as IDEAL PLANT ARCHITECTURE1 (IPA1) or WEALTHY FARMER'S PANICLE (WFP) promotes panicle branching (Jiao *et al.*, 2010; Miura *et al.*, 2010), while FRIZZY PANICLE (FZP), an ethylene-responsive element binding factor, promotes SM identity (Komatsu *et al.*, 2003; Bai *et al.*, 2016). While most reported mutations in master regulatory genes negatively affect panicle development and floral fertility, mutations that increase OsSPL14 or reduce FZP amounts can have significant beneficial effects to improve rice productivity (Jiao *et al.*, 2010; Zhang *et al.*, 2017; Huang *et al.*, 2018).

The phosphatidylethanolamine-binding proteins (PEBP) family also affects panicle development, and consists of three main subfamilies: *FLOWERING LOCUS T* (*FT*)-like, *MOTHER OF FT AND TFL1* (*MFT1*)-like, and *TERMINAL FLOWER1* (*TFL1*)/ *CENTRORADIALIS* (*CEN*)-like genes (Chardon & Damerval, 2005). There are 19 *PEBP*-like genes in rice, including 13 *FT*-like genes, two *MFT*-like genes, and four *TFL1/CEN*-like genes named *RICE CENTRORADIALIS 1* (*RCN1*) to *RCN4* (Chardon & Damerval, 2005; Danilevskaya *et al.*, 2008). Panicles overexpressing *RCN1*, *RCN2*, or *RCN3* exhibit a more highly branched, denser morphology owing to a delayed phase transition from IM to SM (Nakagawa *et al.*, 2002; Zhang *et al.*, 2005). Conversely, knocking down simultaneously all *RCN* genes caused much reduced panicles (Liu *et al.*, 2013; Kaneko-Suzuki *et al.*, 2018).

Rice also has five *SEPALLATA* (*SEP*) subfamily MADS-box genes required for spikelet and flower development: *OsMADS1*/ *LEAFY HULL STERILE1* (*LHS1*), *OsMADS5*, and *OsMADS34*/ *PANICLE PHYTOMER2* (*PAP2*) are paralogous members of the *LOFSEP* clade; while *OsMADS7* (allelic to *OsMADS45*) and *OsMADS8* (allelic to *OsMADS24*) belong to the *SEP3* clade (Malcomber & Kellogg, 2005; Zahn *et al.*, 2005; Arora *et al.*, 2007). Rice *LOFSEP* genes specify the identity of the SM and of the lateral organs it produces, i.e. the rudimentary glumes, sterile lemmas, lemma, and palea. *LOFSEP* and *SEP3* genes are then both required to specify FM and floral organ identity (Jeon *et al.*, 2000; Prasad *et al.*, 2001, 2005; Agrawal *et al.*, 2005; Cui *et al.*, 2010; Wang *et al.*, 2010; Khanday *et al.*, 2013; Zhang *et al.*, 2013; Hu *et al.*, 2015; Wu *et al.*, 2018). Only *OsMADS34/PAP2* has been implicated in panicle development, with a role in specifying IM development downstream of the rice FT-like florigens, and in promoting the transition from PBMs/SBMs to SMs (Gao *et al.*, 2010; Kobayashi *et al.*, 2010, 2012). Loss of *OsMADS34/ PAP2* function increases primary branching, but there is some disagreement about its effect on secondary branches and spikelets as *osmads34* mutation causes secondary branch abortion (Gao *et al.*, 2010; Kobayashi *et al.*, 2010).

In this study, we present a rigorous evaluation of panicle architecture phenotypes, focussing on the roles of *OsMADS5* and *OsMADS34* during inflorescence development. We have used single and double loss-of-function mutants, and overexpression constructs, to demonstrate the effect of these genes on panicle branching, and identify the *TFL1*-like gene *RCN4* as a direct downstream target of both OsMADS5 and OsMADS34 proteins. Our results reveal that *OsMADS5* and *OsMADS34* cooperatively regulate panicle branching in rice by modulating *RCN4* activity, while they promote rachis and branch elongation through a *RCN4*-independent mechanism.

Materials and Methods

Plant materials and growth conditions

Rice (*Oryza sativa* ssp. *japonica*) variety 9522 was used as the wild-type (WT) and the background for all subsequent mutations. The *osmads34-1* single mutant of the variety 9522 has been previously described by our group (Gao *et al.*, 2010). We have previously described also the *osmads5(M)-*, *osmads5(I)-* and *osmads34(I)-CRISPR* mutagenesis (Wu *et al.*, 2018). The four *osmads5* knockout alleles generated in this study in both 9522 WT and *osmads34-1* background are shown in Supporting Information Fig. S1. The *rcn4* single mutant, and *rcn4 osmads34-1* double mutant were obtained using CRISPR/Cas9 technology as previously described (Zhang *et al.*, 2014). Therefore, all the single and higher-order mutants presented in this study were in variety 9522. Primers used for constructing single guide RNA (sgRNA) and overexpression vectors are listed in Table S1. Plant genotyping was performed by PCR-amplification of the regions carrying the mutations, and sequencing the PCR products. The primers used for PCR are listed in Table S1.

All plants were cultivated in the paddy field of Shanghai Jiao Tong University under natural growing conditions from May to September.

To construct overexpression vectors for *OsMADS5*, *OsMADS34* and *RCN4*, RNA from the 9522 inflorescence at stage In5 was isolated, and complementary DNA (cDNA) generated as previously described (Li *et al.*, 2006). Coding sequences for the three genes were amplified (primers in Table S1) and cloned into the overexpression vector *PTCK303* under control of the *Ubiquitin* promoter (*pUbi*) using the In-Fusion HD Cloning Kit (Takara, Shiga, Japan) and sequenced (BGI, Beijing, China). Overexpression constructs were introduced into 9522 calli using *Agrobacterium*-mediated transformation and selection by hygromycin B, following Hiei *et al.* (1994).

A total of 24 and 17 T_0 lines were obtained and observed for *pUbi::OsMADS5* in 9522 and *pUbi:OsMADS34* in 9522, respectively, and three lines from each population were chosen for further analysis based on high levels of transgene expression in panicle primordia (Figs S2, S3). For *pUbi::RCN4* in 9522, 14 T_0 lines were obtained, and two lines with representative phenotypes and high levels of transgene expression in panicle primordia (Fig. S4) were chosen for further analysis.

For each experiment and plant line, only the panicle from the main shoot was used for analysis.

Complementation of the *osmads34-1* mutant

The WT genomic fragment of *OsMADS34*, containing the 3108 bp promoter sequence upstream of the start codon and the

6101 bp genomic fragment containing the *OsMADS34* gene coding sequence (eight exons and seven introns) minus the stop codon, was amplified using the primers *OsM34* gDNA-1F and *OsM34* gDNA-1R (Table S1). *OsMADS34* gDNA was first cloned into *pDONR207* (Invitrogen) using Gateway BP clonase II mix (Invitrogen), and then introduced into the Gateway vector *pK7FWG,0* from VIB-UGent (Karimi *et al.*, 2002) using Gateway LR clonase II mix (Invitrogen). From this vector, the full-length fragment of *OsMADS34* gDNA plus *eGFP* (enhanced green fluorescent protein) was amplified with primers *OsM34* Pro-gDNA-GFP-1F and *OsM34* Pro-gDNA-GFP-1R (Table S1) and cloned into the *Bam*HI and *Bst*ÆII sites of *pCAMBIA1301*, thus replacing the *CaMV 35S* promoter and all the other sequences before the NOS polyadenylation signal, to generate *pOsMADS34::gOsMADS34-GFP*. The constructed vector was introduced into *osmads34-1* calli using the *Agrobacterium*-mediated transformation method (Hiei *et al.*, 1994). Regenerated plants were confirmed to carry the *osmads34-1* mutation by sequencing the PCR product from primers JD M34-GFP-1F and JD M34-GFP-1R (Table S1).

A total of 29 T0 lines expressing *pOsMADS34::gOsMADS34-GFP* in the *osmads34-1* background were obtained, of which 27 lines rescued completely the *osmads34-1* phenotype. Preliminary Western blot experiments were carried out to confirm the expression of the OsMADS34-GFP fusion protein and its expected size (Fig. S5), using young panicle chromatin samples from successful complementation lines (Fig. S6) and the Western blot protocol later. We selected one T3 independent line that carried a single, homozygous copy of the *OsMADS34-GFP* transgene for further analysis.

Western blotting

OsMADS34-GFP was detected using the GFP polyclonal antibody (Invitrogen). Chromatin from WT or *pOsMADS34::gOsMADS34-GFP osmads34-1* young panicles was prepared as described for the chromatin immunoprecipitation-quantitative polymerase chain reaction (ChIP-qPCR) assay (see later). After centrifuging at 16 000 *g* at 4°C for 5 min, the supernatant was separated by 10% sodium dodecyl sulphate-polyacrylamide gel electrophoresis (SDS-PAGE) gel. Proteins were blotted onto a nitrocellulose membrane, detected by a 1 : 3000 GFP polyclonal antibody dilution, with the goat anti-rabbit secondary antibody at a dilution of 1 : 5000, and visualized with Omni-ECL Pico Light Chemiluminescence Kit (Epizyme Biomedical Technology, Shanghai, China).

Confocal imaging

To observe OsMADS34-GFP fluorescence, transgenic shoot apices and young inflorescences at different stages were embedded in 4% (w/v) low melting agarose and sliced into 50 μm thick sections using Leica Vibratome VT1000S as described by Fang *et al.* (2020). Fluorescent and bright field images were taken on a TCS SP5 confocal microscope (Leica, Wetzlar, Germany). GFP signal was imaged using 488 nm excitation and 505–530 nm emission.

Microscope and image processing

Fresh young panicles were fixed in FAA (50% ethanol, 3.5% formalin and 5% acetic acid) for 24 h. For clearing, after dehydration in a graded ethanol series, samples were transferred into benzyl-benzoate-four-and-a-half fluid (Herr, 1982). The cleared samples were observed using a microscope (Eclipse 80i; Nikon, Tokyo, Japan) that was equipped with Nomarski differential interference contrast optics. Samples for scanning electron microscopy (SEM) were prepared and observed as described by Li *et al.* (2006).

Quantitative reverse transcription-polymerase chain reaction

Total RNA from three biological replicates of young panicles (stages In2–In6) and leaves was extracted using Trizol reagent (Invitrogen), according to the manufacturer's instructions. The cDNA was synthesized using the FastQuant RT Kit with gDNase (Tiangen Biotech, Beijing, China). Quantitative reverse transcription polymerase chain reaction (qRT-PCR) was performed in triplicate using the LightCycler 96 Real-Time PCR System (Roche, Basel Switzerland) with QuantiNova SYBR Green PCR Kit (Qiagen, Hilden, Germany) using primers as described in Table S1. The *OsActin* gene (LOC_Os03g50885) was used to normalize expression levels.

In situ hybridization

Fresh young panicles (stages In1–In6) were harvested and immediately fixed in FAA solution, dehydrated, infiltrated, and embedded in paraffin (Wu *et al.*, 2018). Probes were labelled with digoxigenin using the DIG RNA Labelling Kit (SP6/T7; Roche) and primers in Table S1. Pre-treatment of sections, hybridization, and digoxigenin signal detection were performed following Dreni *et al.* (2007). Images were obtained using a Nikon microscope (Eclipse 80i).

Bimolecular fluorescence complementation assay

The bimolecular fluorescence complementation (BiFC) assay was performed in *Nicotiana benthamiana* leaves, following Mao *et al.* (2020). The cDNAs of *OsMADS5* and *OsMADS34* were amplified (primers in Table S1) and cloned into both *pXY104* and *pXY106* vectors, which contained C- and N-terminal domain of yellow fluorescent protein (cYFP and nYFP, respectively). Vectors were introduced in combination into *Agrobacterium tumefaciens* GV3101, and transiently expressed in *N. benthamiana* leaves for 48 h. YFP signal was imaged using 514 nm excitation and 525–555 nm emission using a Leica TCS SP5 confocal microscope.

Dual-luciferase assay

The dual-luciferase (LUC) transactivation assay was performed in *N. benthamiana* leaves, following Tao *et al.* (2018) with six biological replicates. To prepare the *pGreenII-0000-VP16*

effector vector, the coding region of the Herpes Simplex Virus VP16 activation domain was artificially synthesized and cloned into *pGreenII-0000*. The effector plasmids *35S::OsMADS5* and *35S::OsMADS34* were prepared by cloning the full length cDNAs of *OsMADS5* and *OsMADS34* from cDNA used for qRT-PCR analysis. Coding sequences were cloned into both *pGreenII-0000* and *pGreenII-0000-VP16*, such that constitutive *OsMADS* expression was driven by the *CaMV 35S* promoter, with *VP16* (if present) fused at their 3′. The empty vector *pGreenII-0000* was used as the negative control. The reporter *pRCN4::LUC* was constructed by cloning the 3665 bp *RCN4* promoter sequence upstream of the start codon into the vector *pGreenII-0800-LUC* to drive LUC expression. Primers used to amplify coding sequences are listed in Table S1.

Effectors and reporters were introduced in combination into *A. tumefaciens* GV3101, and then into 28-d old *N. benthamiana* leaves, following Li *et al.* (2014). LUC and REN activities were measured using the Dual-Luciferase reporter kit (Promega, Madison, WI, USA). The LUC : REN ratio was measured in a GloMax 20/20 luminometer (Promega). Six biological replicates were used for each experiment. Primers are available in Table S1.

Chromatin immunoprecipitation-quantitative polymerase chain reaction

The ChIP assay was performed according to Bowler *et al.* (2004) with minor modifications. Approximately 1 g of inflorescence < 5 mm in length from WT or *pOsMADS34::gOsMADS34-GFP osmads34-1* complemented plants was crosslinked by 1% (v/v) formaldehyde in extraction buffer (0.4 M sucrose, 10 mM Tris-HCl, 5 mM β-mercaptoethanol, 0.1 mM PMSF and protease inhibitor cocktail, pH 8.0) and ground in liquid nitrogen. Subsequently, the chromatin was isolated and sonicated to yield DNA fragments of 200 to 500 bp in length. The GFP-Trap Magnetic Agarose (ChromoTek, Munich, Germany) was used to precipitate the OsMADS34–DNA complexes. *RCN4* promoter fragments were quantified by qRT-PCR as described earlier (Li *et al.*, 2011) using primers listed in Table S1, and enrichment in M34-GFP samples was compared to levels in WT plants.

Electrophoretic mobility-shift assays

The full-length cDNAs of *OsMADS5* and *OsMADS34* were cloned into the vector *pGADT7* (Clontech, TaKaRa, Shiga, Japan) for *in vitro* transcription/translation (TNT T7/SP6 Coupled Wheat Germ Extract System; Promega). Fluorescein amidite (FAM)-labelled probes were generated by annealing two complementary primers containing FAM at the 5′-end. The binding reaction mixture contained 25 mM Tris-acetate (pH 7.5), 1 mM DTT, 0.1 mg ml^{-1} BSA, 2 mM MgAc, 20 nM FAM-labelled DNA, and 3 μl of *in vitro* synthesized protein. The binding reaction was performed for 30 min at 25°C before loading on a 6% native polyacrylamide gel. Competition was tested using 100-fold excess of nonlabelled probes. FAM-labelled probes were visualized using the FAM channel of a ChemiDoc MP imaging system (Bio-Rad, Hercules, CA, USA). Primers are listed in Table S1.

Statistical analysis

The one-way analysis of variance (ANOVA, $P < 0.05$) and Students *t*-tests ($P < 0.05$, $P < 0.01$, and $P < 0.001$) were run with Pasw statistics 18 (IBM, Armonk, NY, USA). All data are shown as means ± SD ($n \geq 3$).

Accession numbers

The sequences for all the genes mentioned in this article are available in the Rice Genome Annotation Project Database (http://rice.plantbiology.msu.edu/) with the following accession numbers: *OsMADS5* (LOC_Os06g06750), *OsMADS34* (LOC_Os03g54170), *RCN1* (LOC_Os11g05470), *RCN2* (LOC_Os02g32950), *RCN3* (LOC_Os12g05590), and *RCN4* (LOC_Os04g33570).

Results

Expression of *OsMADS5* and *OsMADS34* at panicle initiation

The spatio-temporal expression patterns of *OsMADS5* and *OsMADS34* were analysed throughout early inflorescence development by *in situ* RNA hybridization (Figs 1a, S7). *OsMADS5* expression was almost undetectable in the IM and primary branch primordia until stage In4, after which *OsMADS5* was expressed highly in SBMs and SMs (stages In5 and In6), as previously reported (Kobayashi *et al.*, 2010; Wu *et al.*, 2018). *OsMADS34* transcript appeared in the apical IM at stage In1, and was expressed consistently in the initiating PBM, SBM, and SM throughout inflorescence development, consistent with previous results (Gao *et al.*, 2010; Kobayashi *et al.*, 2010; Wu *et al.*, 2018). *OsMADS34* expression thus dominates over *OsMADS5* until stage In4, after which the two genes share a similar expression profile.

We further characterized *OsMADS34* expression by analysing the spatio-temporal distribution of its GFP-tagged protein under control of its native promoter. A reporter construct containing the *OsMADS34* promoter and genomic sequence, fused in frame with *GFP*, was introduced into *osmads34-1* calli (hereafter referred to *osmads34*; Gao *et al.*, 2010). The mutant inflorescence, branch, and spikelet phenotypes of *osmads34* were fully rescued in the transgenic plants, indicating that OsMADS34-GFP is biologically functional (Fig. S6). GFP fluorescence was not detected in the SAM at the vegetative stage, nor in the stem parenchyma and pro-vasculature underlying the SAM (Fig. 1b). Upon transition to reproductive development (stage In1), GFP fluorescence was clearly visible throughout the elongating IM, which extended to developing PBMs at stages In2, In3, and In4, the newly formed SBMs at stage In5, and the developing SBMs at stage In6. OsMADS34-GFP localized in the nuclei (Figs 1b, S7). These results indicate that the OsMADS34 protein persists in meristems throughout inflorescence development, consistent with the *in situ* hybridization results (Fig. 1a) and previous studies on the distribution of *OsMADS34* transcript (Gao *et al.*, 2010; Kobayashi *et al.*, 2010, 2012; Meng *et al.*, 2017).
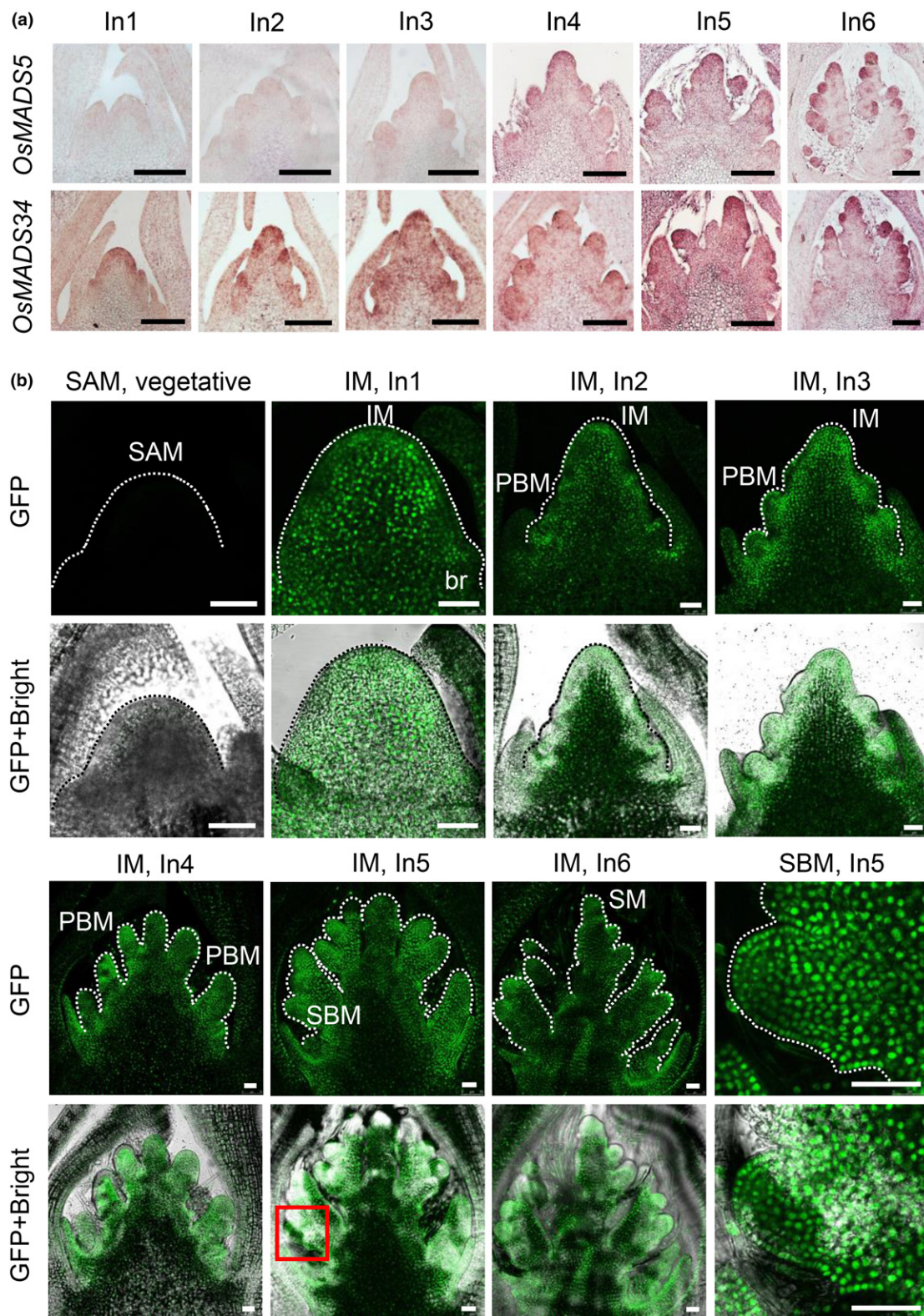
Fig. 1 Expression of *OsMADS5* and *OsMADS34* in the developing rice inflorescence. (a) *In situ* RNA hybridization of *OsMADS5* (upper) and *OsMADS34* (lower) in the wild-type inflorescence at stages In1–In6. Bar, 100 μm. (b) Confocal images (green fluorescent protein (GFP) only or GFP + bright field merge) of transgenic plants expressing the *pOsMADS34::gOsMADS34-GFP* reporter gene: the shoot apex meristem (SAM) at the vegetative stage; the inflorescence meristem (IM) at stages In1, In2, In3, In4, In5, and In6, indicating emergence of primary branch meristems (PBMs), secondary branch meristems (SBMs), and spikelet meristems (SMs); an enlargement of an SBM at In5 (red box from IM image). Bar, 50 μm.

OsMADS5 and OsMADS34 redundantly regulate inflorescence architecture

The effect of *OsMADS34* in panicle architecture was examined using an existing *osmads34* mutant (Gao *et al.*, 2010). Extensive abortion of branches and spikelets was observed in the basal nodes in the dense mutant panicle, whose small white vestigials were still visible at the heading stage (Fig. 2a,b). Once these arrested organs were carefully dissected under the stereomicroscope and included in the total count, *osmads34* panicles displayed more primary, secondary, and even tertiary, branches compared with the WT panicle (Fig. 2c). This phenotype was consistent with the description of the *pap2-1* allele from an independent research team (Kobayashi *et al.*, 2010) and we further confirmed it on the *osmads34* knockout mutant that we recently generated using CRISPR/Cas9 system (*osmads34(I)-CRISPR*; Wu *et al.*, 2018; Fig. S8). Both the numbers of secondary branches per panicle and per primary branch increased in *osmads34* mutants (Figs 2c, S8b), demonstrating that the increase in secondary branch number is not simply due to an increase in primary branch numbers. Thus, the activities of both the IM and lateral branching meristems are significantly increased in *osmads34* panicles.

Since *OsMADS5* is co-expressed with its paralogue *OsMADS34* at the SBM stage (stages In5 and In6, Fig. 1a), we also hypothesized a role of *OsMADS5* in inflorescence branching (Fig. 2). We extended the CRISPR-Cas9 mutagenesis targeting the first and second exons of *OsMADS5* that we described recently (Wu *et al.*, 2018), and we obtained four knockout alleles in this work, in both 9522 WT and *osmads34* single mutant backgrounds (Fig. S1), to examine their branching pattern in detail (for simplicity, they will be referred as *osmads5* and *osmads5 osmads34* hereafter). The *osmads5* knockout mutants did not show any obvious branching phenotype compared with WT panicles (Fig. 2). The *osmads5 osmads34* panicles had a number of primary branches equivalent to *osmads34* single mutant (Fig. 2c), but compared with the WT and single mutants, the double mutant panicles exhibited significantly enhanced branching, with increased numbers of secondary branches, higher-order branches up to quaternary, and spikelets (mature + arrested) (Fig. 2). The number of secondary branches per primary branch also increased significantly in *osmads5 osmads34* panicle (Fig. 2c). These results reveal a new role for *OsMADS5* in inflorescence development, sharing some functional redundancy with *OsMADS34* to limit the iteration of branch meristem formation and favour their switch to SM identity.

Ectopic expression of OsMADS5 and OsMADS34 inhibits secondary branch formation

Our next step was to examine the phenotype for *OsMADS5* overexpression during inflorescence development. A constitutively expressed *OsMADS5* cDNA was introduced into WT background (Fig. S2). The number of primary branches per panicle after *OsMADS5* OE was comparable to WT, whereas the number of secondary branches and spikelets decreased significantly

(Fig. 3), supporting our hypothesis that *OsMADS5* positively regulates the transition of branch meristems to SM in rice.

For comparison, we also overexpressed *OsMADS34* in the WT background (Fig. S3). The number of primary branches per panicle in *OsMADS34* overexpression lines was comparable to WT plants; however, the number of secondary branches and spikelets decreased significantly, even more than in *OsMADS5* overexpression lines (Fig. 3c). These results are consistent with *OsMADS5* and *OsMADS34* having partially redundant roles in limiting lateral branching by promoting the transition to SM identity.

Knockout of RCN4 can partially restore the osmads34 panicle phenotype

TFL1 family genes are key regulators of inflorescence development, with four members in rice (*RCN1–RCN4*; Nakagawa *et al.*, 2002; Zhang *et al.*, 2005; Liu *et al.*, 2013; Kaneko-Suzuki *et al.*, 2018), and we have previously shown that *RCN4* is highly expressed in *osmads34* inflorescence primordia, compared to WT (Meng *et al.*, 2017). To further explore the regulatory interactions of *OsMADS5/34* and *RCN* genes during early inflorescence development, the expression of all four *RCN* genes was investigated in *osmads* knockout lines (Fig. S9). *RCN1*, *RCN2*, and *RCN3* were generally expressed at similar levels in WT and mutant inflorescences during primary and secondary branch formation. However, *RCN4* was highly upregulated in both *osmads34* lines, more so in the double mutant, and expression continued to increase as development progressed. *In situ* hybridization revealed that *RCN4* transcript was strongly present in secondary branch primordia of *osmads34*, but not WT, panicles (Fig. 4a), confirming that the dramatic increase of *RCN4* expression in *osmads34* lines was not simply due to their higher number of meristems. These results suggest that de-repression of *RCN4* is directly linked, rather than incidental, to enhanced branching in *osmads34* lines.

To test the hypothesis that *RCN4* works downstream of *OsMADS34*, and to determine which aspects of the *osmads34* phenotype depend on *RCN4* function, we generated the *rcn4-1* and *rcn4-2* knockout alleles by CRISPR-Cas9, in both 9522 WT and *osmads34* single mutant backgrounds (Fig. S10), to examine their branching pattern in detail (for simplicity, they will be referred to as *rcn4* and *rcn4 osmads34* hereafter). The *rcn4* panicles do not show any obvious phenotype compared to WT (Fig. 4b,c). However, the *rcn4 osmads34* panicles were quite distinct from either WT or *osmads34* panicles. Panicles in the double mutant had a number of primary branches equivalent to *osmads34* panicles (Fig. 4b,c). However, the number of secondary branches per primary branch in *rcn4 osmads34* panicles decreased to a level even lower than WT, tertiary branches did not form, and the overall number of spikelets per panicle fell to below WT levels (Fig. 4c). These results are consistent with expression data (Figs 4a, S9), indicating that *RCN4* acts downstream of *OsMADS34* to trigger lateral branching, and support a genetic model in which *OsMADS34* regulates the transition to SM by repressing *RCN4* expression.
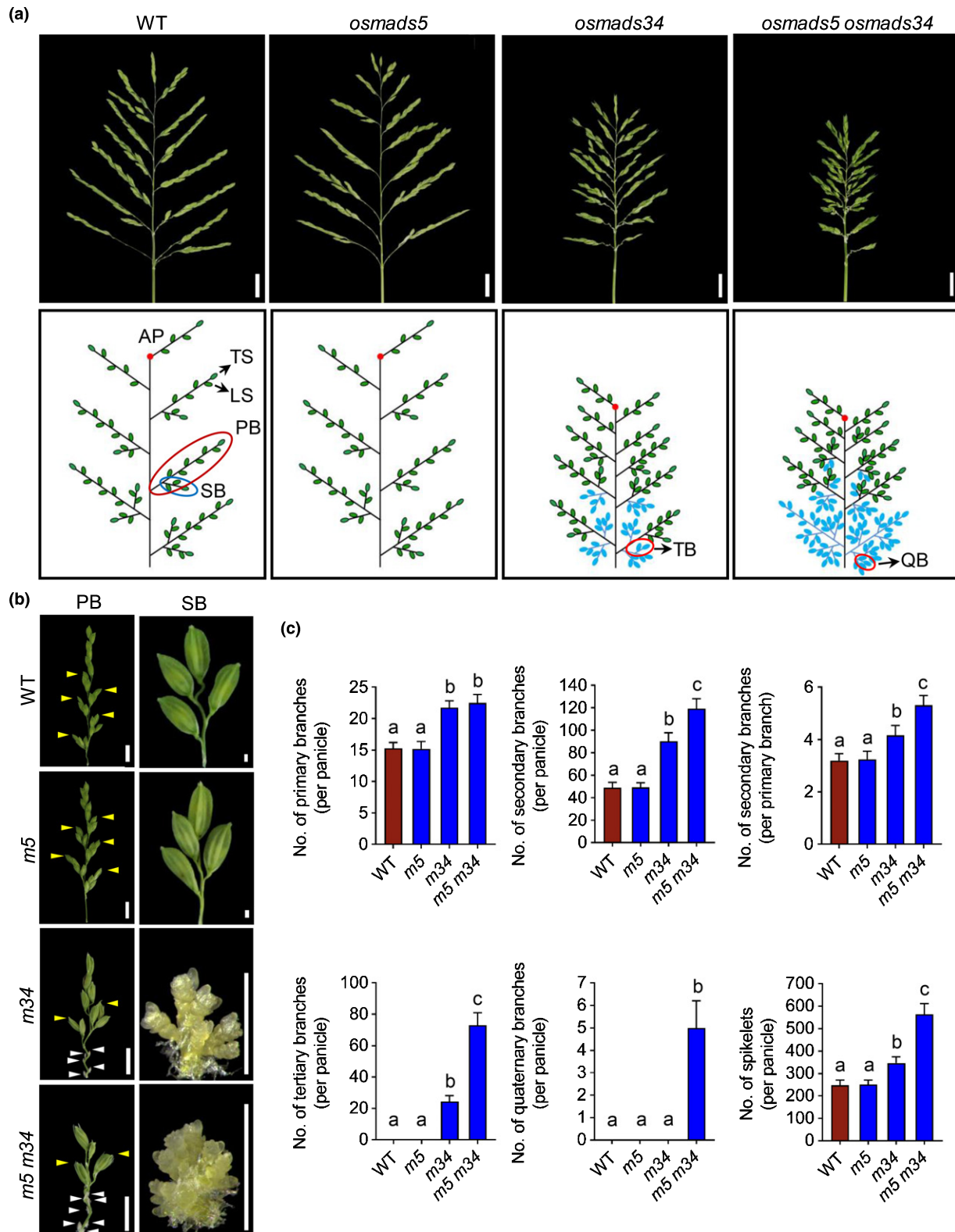
Fig. 2 Branching phenotypes of wild-type (WT), *osmads5* (*m5*), *osmads34* (*m34*), and *osmads5 osmads34* (*m5 m34*) mutants in rice panicle development. (a) The main panicle (upper) and a schematic representation of its structure (lower, inspired by Kyozuka *et al*., 2014), indicating primary branch (PB), secondary branch (SB), tertiary branch (TB), and quaternary branch (QB); terminal spikelet (TS) and lateral spikelet (LS); and arrest point of the inflorescence meristem (AP). Aborted branches and spikelets are shown in blue. Bar, 2 cm. (b) Primary and secondary branches generated from the main panicle. Yellow and white arrowheads indicate the position of normal and aborted SBs, respectively. Aborted SB shown for *m34* and *m5 m34* lines. Bars: 1 cm (PB), 1 mm (SB). (c) Panicle traits, including numbers of PB, SB, TB, and QB per panicle; number of SB per PB; and number of spikelets per panicle. Means ± SD, *n* = 16. Letters indicate significant differences (one-way ANOVA: *P* < 0.05).
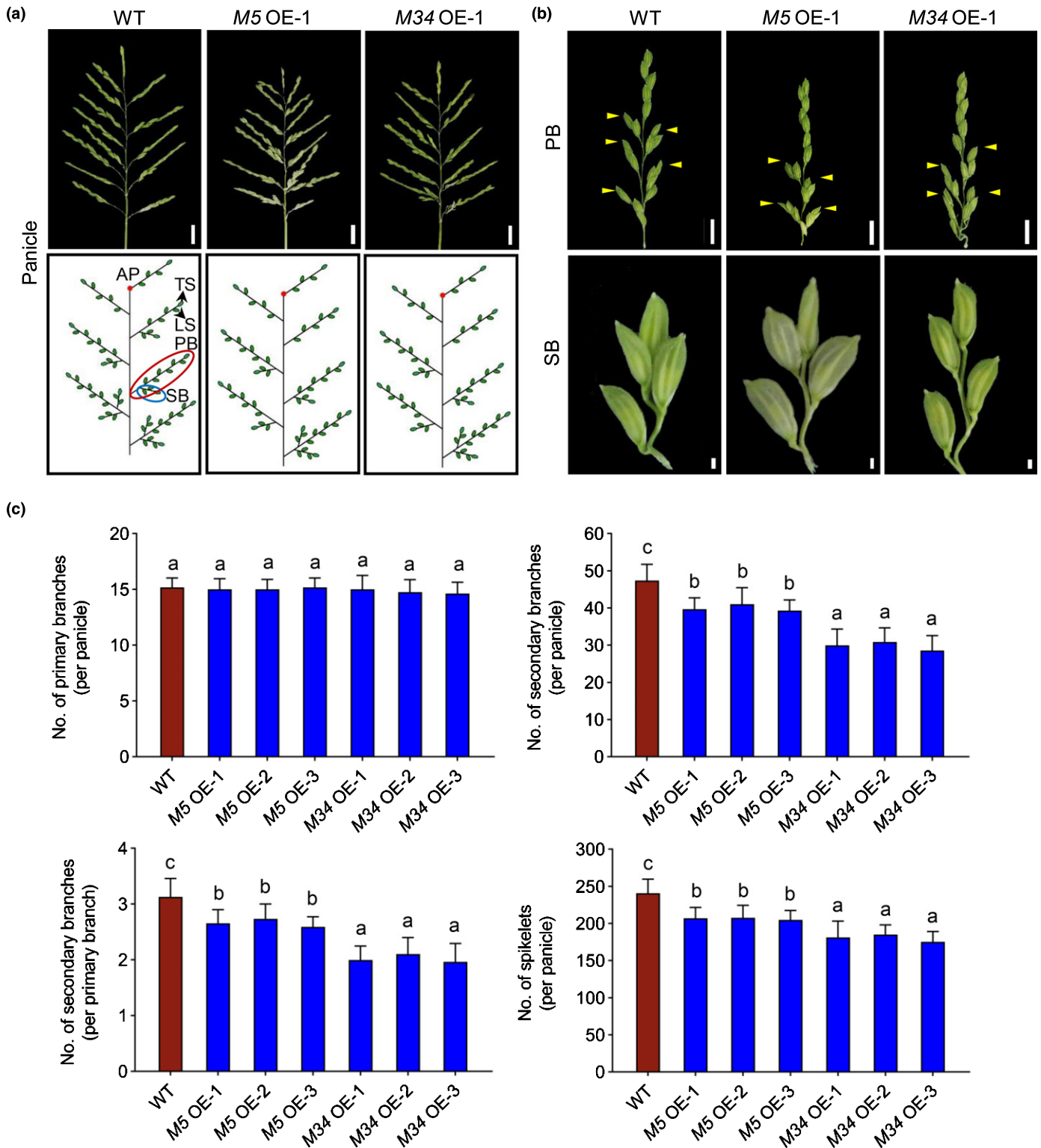
Fig. 3 Effect of *OsMADS5* or *OsMADS34* overexpression (OE) in rice wild-type (WT) plants. (a) The main panicle (upper) and a schematic representation of its structure (lower, inspired by Kyozuka *et al*., 2014), indicating primary branch (PB) and secondary branch (SB); terminal spikelet (TS) and lateral spikelet (LS); and arrest point of the inflorescence meristem (AP). Bar, 2 cm. (b) PB and SB generated from the main panicle. Yellow arrowheads indicate the position of normal SB. Bars: 1 cm (PB), 1 mm (SB). (c) Panicle traits, including numbers of PB and SB per panicle; number of SB per PB; and number of spikelets per panicle. Means ± SD, *n* = 16. Letters indicate significant differences (one-way ANOVA: *P* < 0.05).
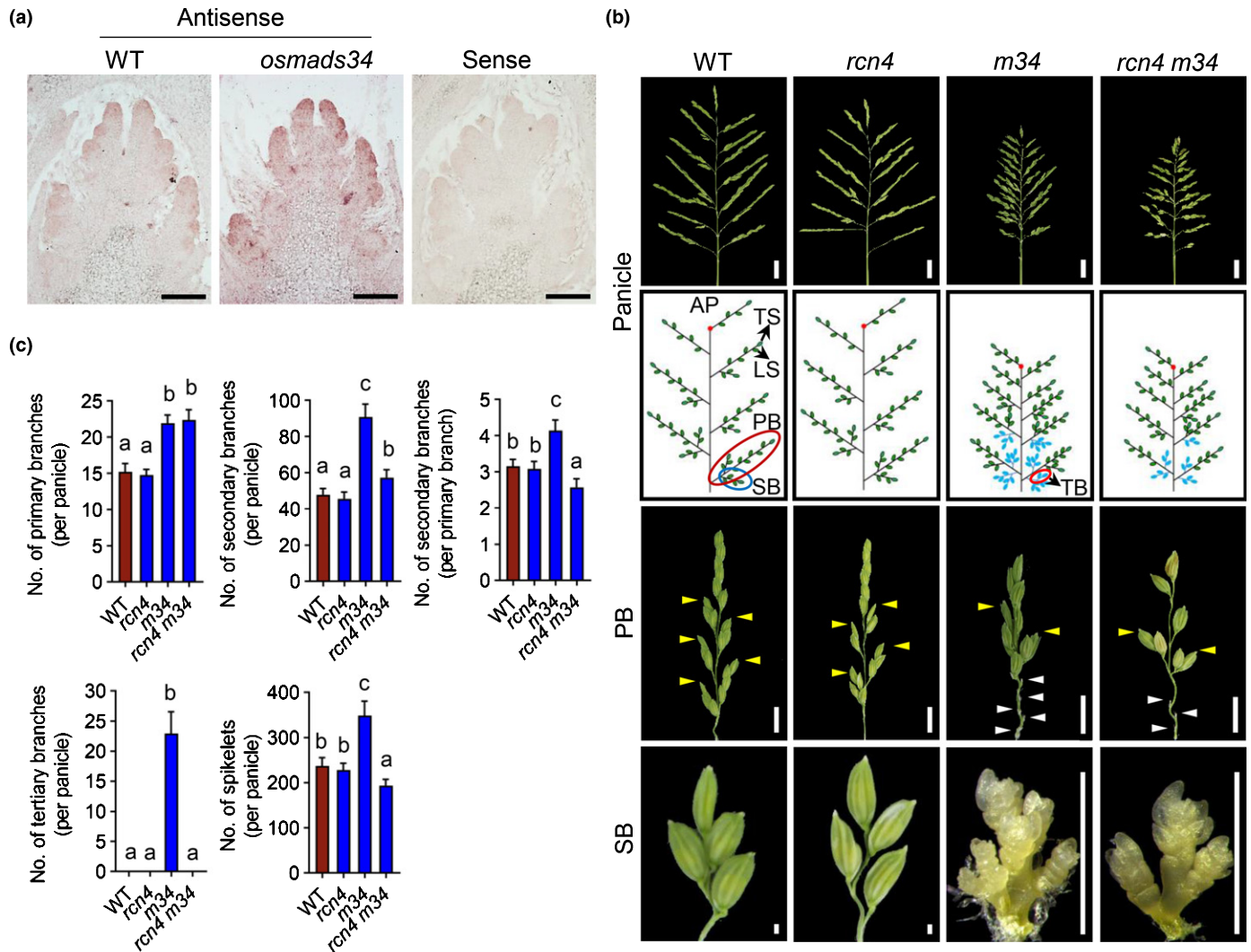
Fig. 4 Phenotype and expression of *RCN4* during rice panicle development. (a) *In situ* hybridization of *RCN4* in wild-type (WT) and *osmads34* IMs at stage In5, with sense control. Bar, 100 μm. (b) The main panicle and a schematic representation of its structure (inspired by Kyozuka *et al*., 2014), indicating primary branch (PB), secondary branch (SB), and tertiary branch (TB); terminal spikelet (TS) and lateral spikelet (LS); and arrest point of the inflorescence meristem (AP). Aborted SBs and spikelets are shown in blue. Bar, 2 cm. Lower panels indicate PB and SB structures. Yellow and white arrowheads indicate the position of normal and aborted SB, respectively. Aborted SB shown for *m34* and *rcn4 m34* lines. Bars: 1 cm (PB), 1 mm (SB). (c) Panicle traits, including numbers of PB, SB, and TB per panicle; number of SB per PB; and number of spikelets per panicle. Means ± SD, $n = 16$. Letters indicate significant differences (one-way ANOVA: $P < 0.05$).

OsMADS34 and OsMADS5 directly bind the *RCN4* promoter

To examine whether OsMADS34 directly regulates *RCN4* expression, we performed ChIP assays using the *pOsMADS34::gOsMADS34-GFP osmads34* complementation plants (Fig. 1b). We analysed the *RCN4* genomic region for CArG box motifs, the canonical binding site for MADS-domain proteins (de Folter & Angenent, 2006), and designed primers to eight regions in *RCN4* regulatory regions: four in the upstream promoter with CArG boxes (C1–C5); two in the second intron with CArG boxes (C6–C8); one in the 3′UTR region with CArG boxes (C9 and C10), and a control region with no CArG box (Fig. 5a). Immuno-precipitation with the anti-GFP antibody revealed enrichment of five CArG-containing regions compared with the WT control (Fig. 5b).

To verify the binding of OsMADS5 and OsMADS34 to these regulatory regions, we performed electrophoretic mobility-shift assays (EMSAs; Fig. 5c). OsMADS5 and OsMADS34 strongly bound to all six probes and competition with nonlabelled probes inhibited binding (Fig. 5c). A dual-LUC assay in tobacco leaves confirmed that OsMADS5 and OsMADS34 could drive LUC expression under control of the *RCN4* upstream promoter when fused to a viral VP16 activation domain (Fig. 5d), confirming a direct interaction between them, but the native OsMADS proteins neither activated nor repressed *RCN4* expression. Together, these results demonstrate that OsMADS5 and OsMADS34 directly bind the promoter and second intron of *RCN4*, but do
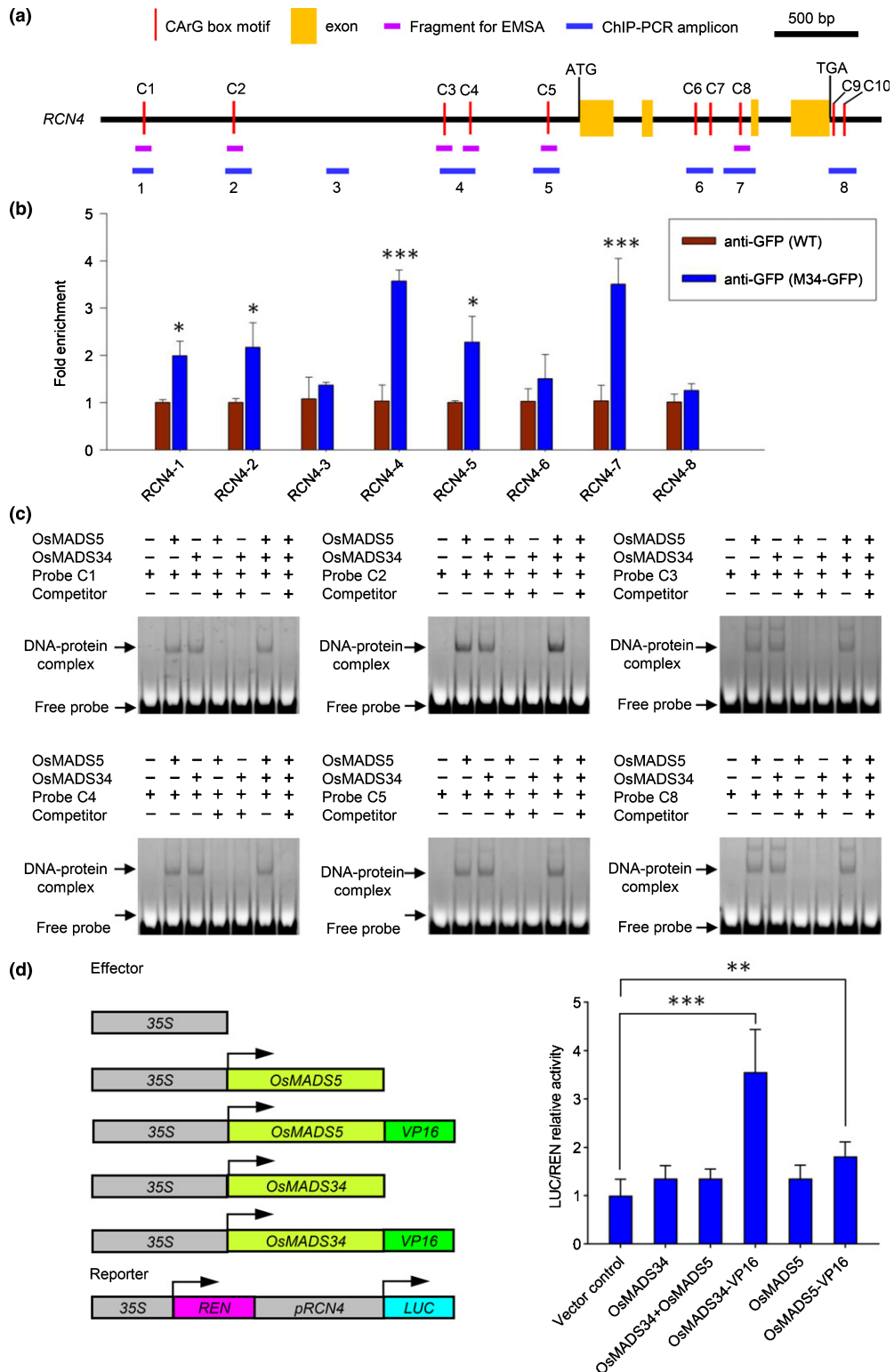
Fig. 5 Binding of rice OsMADS5 and OsMADS34 to the *RCN4* promoter. (a) Schematic representation of the *RCN4* genomic region showing the 10 CArG box motifs, C1–C10. (b) Chromatin immunoprecipitation-quantitative polymerase chain reaction (ChIP-qPCR) results for the eight targeted amplicons. Enrichment was compared with the input sample. Mean ± SD, $n = 3$. (c) Electrophoretic mobility-shift assay (EMSA) using the OsMADS5 and OsMADS34 proteins and fragments of the *RCN4* promoter containing CArG box motifs as probes labelled with 5′-FAM. A 100× excess of nonlabelled probes were used for competition. (d) Transient dual-luciferase (LUC) assays to show OsMADS5 and OsMADS34 binding to the *RCN4* promoter. Constructs are shown in the left panel; the *RCN4* promoter in the reporter construct contains promoter sequence upstream of the start codon. Transcriptional activation of *pRCN4::LUC* by the MADS proteins was effected by conjugation to VP16, a transcriptional activation domain. Means ± SD, $n = 6$. Statistical significance is indicated by: *, $P < 0.05$; **, $P < 0.01$; ***, $P < 0.001$ (Student's t-test).

not affect *pRCN4::LUC* transcription, either due to incomplete inclusion of target CArG motifs in the LUC reporter construct, or because OsMADS proteins act in concert with other proteins to affect gene transcription.

BiFC assays (Fig. S11) and our previous yeast two-hybrid assays (Wu *et al.*, 2018) showed the formation of OsMADS5-OsMADS34 heterodimers and OsMADS34 homodimers, while OsMADS5 homodimerization was only observed in BiFC assays. The lower activation of *pRCN4::LUC* by OsMADS5-VP16 (Fig. 5d) might be related to a weaker ability of OsMADS5 to homodimerize in the tested conditions.

RCN4 overexpression dramatically alters panicle architecture

Constitutive overexpression of *RCN4* in WT plants reduced plant growth and delayed flowering time (Figs S4, S12a). The *RCN4* overexpression plants also produced aberrant florets with smaller palea, lemma, anthers, and malformed carpel with three stigmata (Fig. S12b). The *RCN4* overexpression panicle phenotype was very different compared to WT: while the number of primary branches was similar, the *RCN4* overexpression panicles had a much higher number of secondary and higher-order branches (Figs 6, 7). In WT panicles, a primary branch produces up to five secondary branches, and further branching is never observed (Fig. 6c). In contrast, *RCN4* overexpression panicles produced up to nine secondary branches from a primary branch (Fig. 6b), and the development of tertiary, quaternary, and even quinary, branches was frequently observed (Fig. 6c). Overall, a seven-fold increase in the number of initiated spikelets was observed in *RCN4* overexpression compared with WT panicles (Fig. 6c), although branches and spikelets on the lower part of a panicle often aborted (Figs 6b, 7). These results show that also *RCN4*, like other *RCN* genes, suppresses the transition from branch to spikelet meristem, and its overexpression promotes lateral branching.

Inactivation of *OsMADS5* and *OsMADS34* prolongs secondary branching phase

For the large-scale phenotyping described earlier, branches were dissected and counted at heading stage. To validate our interpretation of the ontogenesis of the white vestigials as true branches, we also analysed panicles directly at the young stage In7. Whole primary branches were visualized after clearing treatment to make bract hairs invisible, while details of secondary branches were imaged by SEM (Fig. 7). We confirmed that SBMs, especially those at the very base of young primary branches near the rachis, acquired a partial indeterminacy and proliferated in *osmads34*, *osmads5 osmads34* and *RCN4* overexpression plants. The resulting structures were clearly identifiable as higher-order branch primordia (Fig. 7). Compared to the distichous pattern of WT, these extra branches developed towards all directions. Furthermore, when the terminal spikelets were visibly synchronous at late stage Sp8 in the primary branches of WT, *osmads34* and *osmads5 osmads34*, the most basal spikelets were already around stage Sp4

in WT; instead, the developmental gap between terminal and basal structures was much increased in the mutants, where basal meristems still at the earlier Sp or even SM stages were observed. This analysis confirms the proposed model of delayed meristem transition caused by the loss of *OsMADS5* and *OsMADS34*.

Along the rachis, the increased SBM proliferation occurred mostly in the basal primary branches of the mutants, with a decreasing gradient towards the rachis apices, and apical primary branches were partially affected only in the *RCN4* overexpression lines (schematics in Figs 2a, 6a).

OsMADS5 and *OsMADS34* promote rachis and primary branch elongation

Despite the robust increase in branching activity, *osmads34* and *osmads5 osmads34* panicles are consistently smaller than WT, with visibly shorter rachis and branches (Fig. 2a). As for inflorescence branching, the *osmads5* single mutant does not affect the process of rachis elongation, while *osmads34* panicles have a shorter rachis with more nodes (Fig. 8a,b). The *osmads5 osmads34* rachis is further shortened, but with the same number of nodes than *osmads34*. In both WT and, more frequently, in these mutants, some rachis internodes do not develop at all, giving the impression of two or three primary branches attached at the same node (Fig. 2a), explaining why the number of apparent rachis nodes is lower than the number of primary branches per panicle (Figs 2c, 8b). In *osmads34*, only the internodes up to position 9 are shorter than WT, and the double *osmads5 osmads34* mutation causes the lengths of the first two basal internodes to reduce even further (Fig. 8c). The longest primary branches are those in position 2–6 in WT and 6–12 in *osmads34*, while primary branch length is strikingly consistent in the *osmads5 osmads34* mutant panicle (Fig. 8d).

The effect of *OsMADS5* overexpression is also interesting, as it does not modify the number of primary branches (Fig. 3c) or rachis nodes (Fig. 8b), but decreases the rachis length (Fig. 8a), mostly at the first two internodes (Fig. 8e). In addition, *OsMADS5* overexpression reduces primary branch length, except terminal ones (Fig. 8f). Furthermore, *OsMADS34* overexpression reduces the length of rachis and primary branches more than *OsMADS5* overexpression (Fig. 8a,f). Taken together, these observations indicate that the effect of *OsMADS34* in rachis and primary branch elongation is higher than that of *OsMADS5*, consistent with the gene expression patterns (Fig. 1).

Loss of *RCN4* function had almost no effect on the WT and *osmads34* panicle elongation (Figs 4, 8a,b,g,h), except for the subtle decrease of primary branch length in *rcn4* compared with WT (Fig. 8h) and subtle increase of the rachis nodes number in *rcn4 osmads34* compared with *osmads34* (Fig. 8b). Although *RCN4* overexpression produced more compact panicles, and more compact plants in general, than WT (Figs 6a,c, 8a,b,g,h, S12), the loss of its function do not rescue the rachis and primary branch elongation in *osmads34* mutants. Taken together, these data show that *RCN4* repression by *OsMADS34* primarily functions to counterbalance SBM identity and promote meristem transition to SM identity.
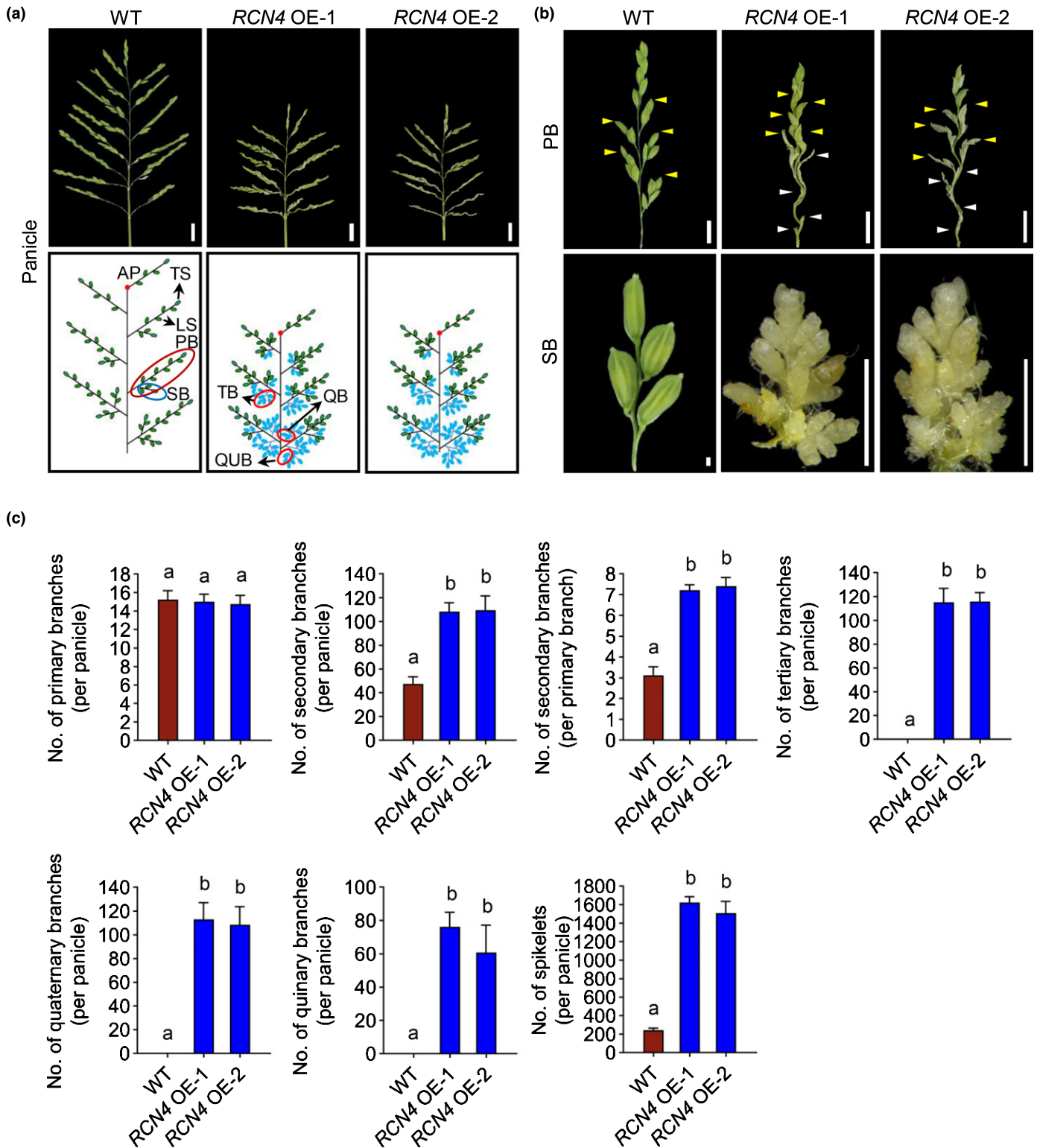
Fig. 6 Effect of *RCN4* overexpression (OE) in rice wild-type (WT) plants. (a) The main panicle (upper) and a schematic representation of its structure (lower, inspired by Kyozuka *et al*., 2014), indicating primary branch (PB), secondary branch (SB), tertiary branch (TB), quaternary branch (QB), and quinary branch(QUB); terminal spikelet (TS) and lateral spikelet (LS); and arrest point of the inflorescence meristem (AP). Aborted branches and spikelets are shown in blue. Bar, 2 cm. (b) PB and SB generated from the main panicle. Yellow and white arrowheads indicate the position of normal and aborted SB, respectively. Aborted SB shown for *RCN4* OE lines. Bars: 1 cm (PB), 1 mm (SB). (c) Panicle traits, including numbers of PB, SB, TB, QB, and QUB per panicle, and number of spikelets per panicle. Means ± SD, $n = 4$. Letters indicate significant differences (one-way ANOVA: $P < 0.05$).
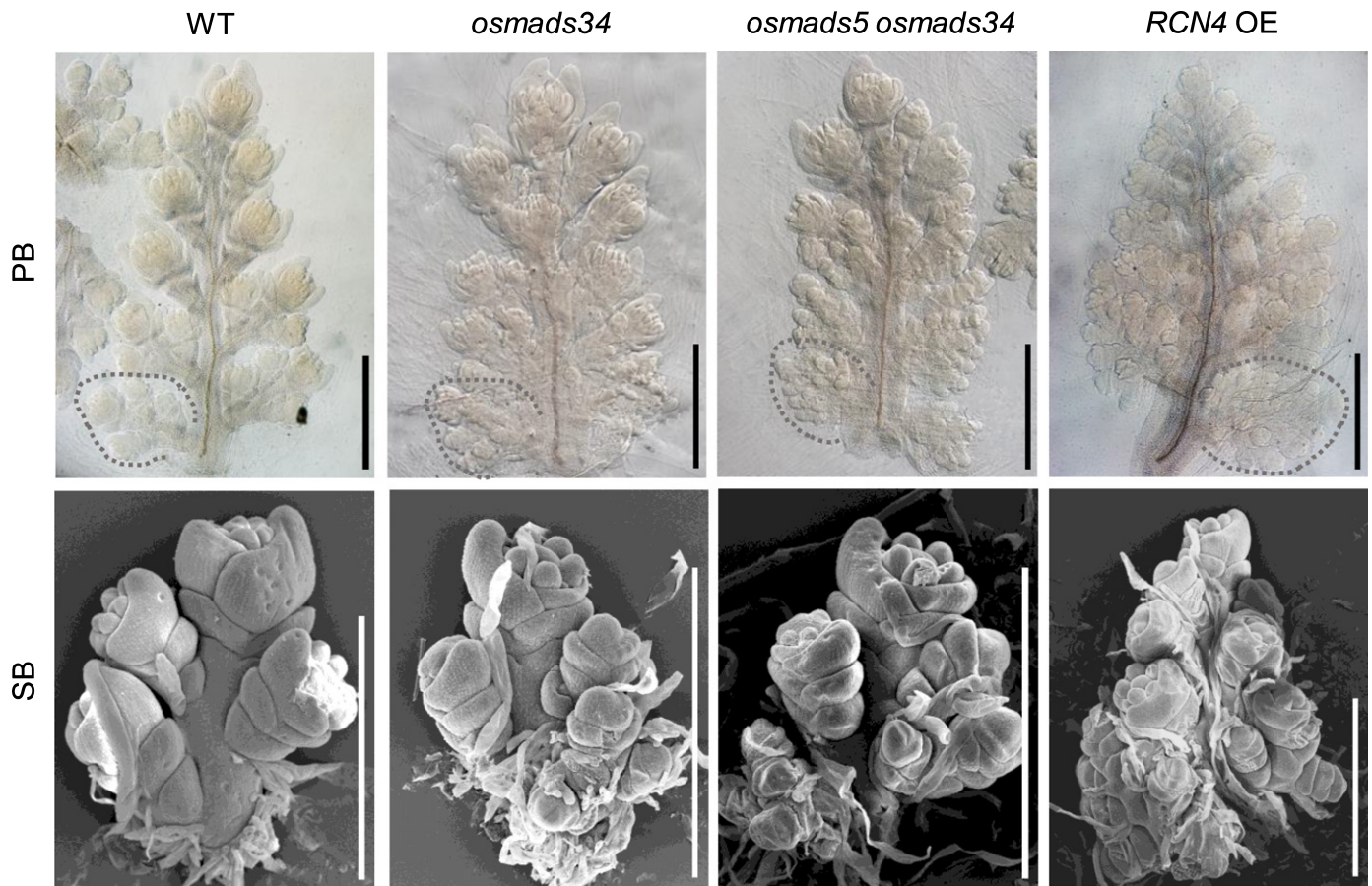
Fig. 7 Views of basal primary branches (PBs) after clearing treatment, and scanning electron microscopy analysis of their secondary branches (SBs, encircled by grey dotted line in PB images) of wild-type (WT), *osmads34* and *osmads5 osmads34* mutants, and *RCN4* overexpression (OE) line at stage In7 in rice. Bar, 500 μm.

Discussion

OsMADS5 and OsMADS34 limit panicle branching by promoting spikelet meristem identity

Rice *SEP* subfamily genes show diverse spatial and temporal expression patterns (Kobayashi *et al.*, 2010). *OsMADS34* expression begins first, at the reproductive transition of the SAM (stage In1, Fig. 1a), and the OsMADS34 protein accumulates in the IM and branch meristems during early inflorescence development (Fig. 1b). *OsMADS5* transcription begins at stage In5, when secondary branches begin to form, and overlaps with *OsMADS34* expression, especially in the SBM and SM (Fig. 1a; Wu *et al.*, 2018). Previous studies have shown that *OsMADS34* plays a positive role in the establishment of SM identity (Gao *et al.*, 2010; Kobayashi *et al.*, 2010, 2012), and here, we have shown that *OsMADS5* is also an important regulator of panicle architecture. Its function is partially redundant with *OsMADS34*, and the *osmads5 osmads34* double mutant showed significantly enhanced panicle branching, up to the fourth order, compared to WT and single mutant plants (Fig. 2).

While *OsMADS34* seems to be the more important gene in determining panicle architecture, it is important to notice that

OsMADS5 is downregulated about three-fold in *osmads34* branch meristems (Fig. S2), which likely contributes to the *osmads34* lateral branching phenotype; and suggests that *OsMADS34* may act upstream of *OsMADS5* to regulate its expression, which would be consistent with the timing of expression of these two genes (Fig. 1). Our loss-of-function and overexpression experiments also show that *OsMADS5* and *OsMADS34* both contribute to regulate rachis and branch elongation (Fig. 8). Transcripts of both genes, and the OsMADS34-GFP protein, accumulated in the forming rachis and branch axes as well as in meristems (Fig. 1), so *OsMADS* genes may have other, cell type–autonomous functions independent of stimulus from meristems. While some genetic factors that interact with *OsMADS34* (*PAP2*) have been identified (*FUL*-like genes (Kobayashi *et al.*, 2012) and *LAX1* (Meng *et al.*, 2017)), further research will be required to understand how *OsMADS34* interacts with other pivotal genes like *FZP* and *IPA1* to shape rice panicle formation.

The remaining *LOFSEP* gene, *OsMADS1*, is unlikely to participate in determining panicle architecture since it activates only from the SM stage (Prasad *et al.*, 2001, 2005; Kobayashi *et al.*, 2010) and, indeed, is used as a marker of SM identity in various *Oryza* species (Ta *et al.*, 2016). Then, a hierarchy in the activation of *LOFSEP* genes, *OsMADS34 > OsMADS5 > OsMADS1*,
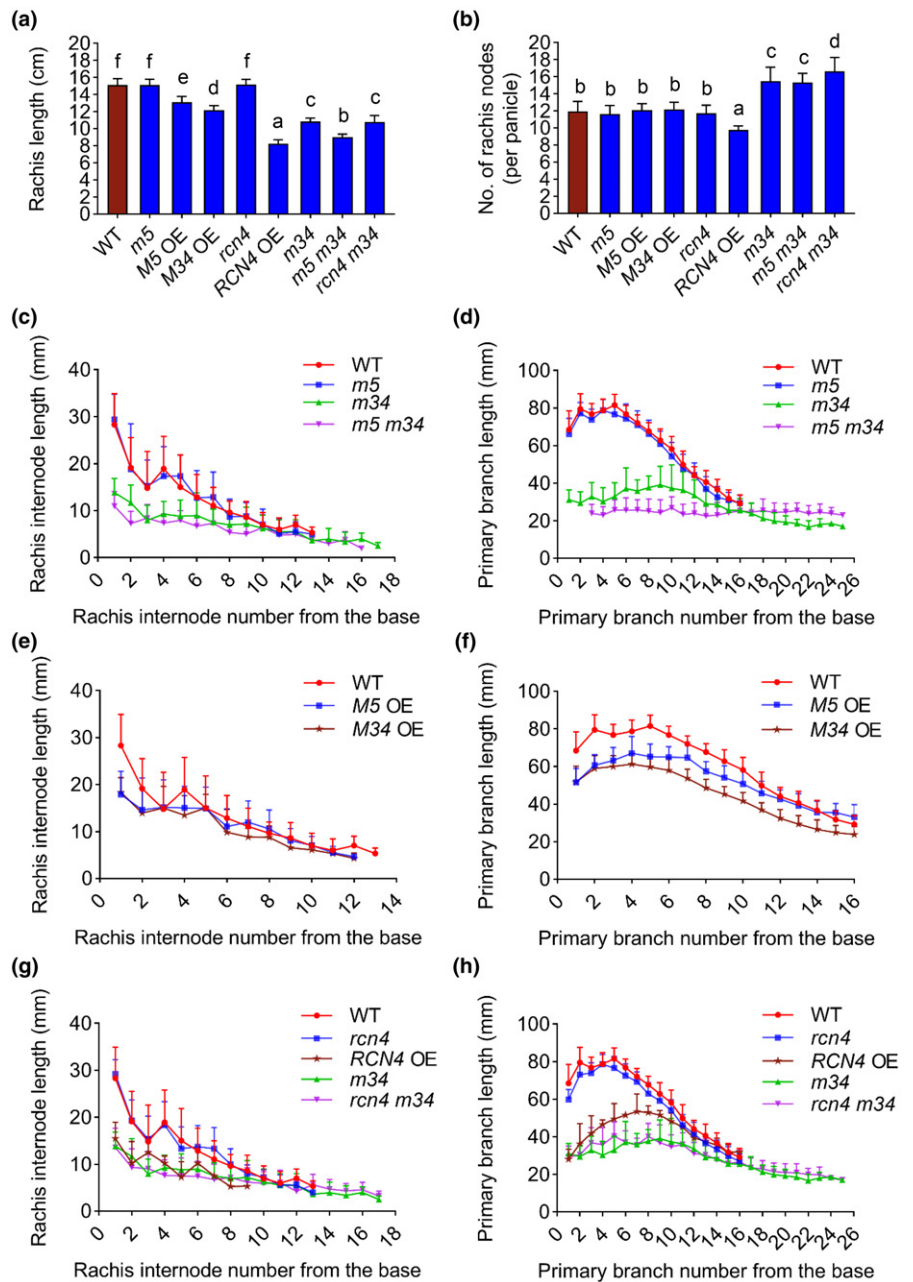
Fig. 8 Rachis and primary branch traits of wild-type (WT) and mutant (knockout and overexpression) *OsMADS5*, *OsMADS34*, and *RCN4* lines in rice. (a, b) Rachis length and number of rachis nodes per panicle for all WT, single, and double mutants generated in this study. Letters indicate significant differences (one-way ANOVA: $P < 0.05$). (c–h) Lengths of rachis internodes and primary branches for all lines. Means ± SD, $n = 4$ for *RCN4* overexpression (OE), $n = 16$ for all other lines.

bears close association with the progression of identity transition in rice reproductive meristems. Once SM identity is established (stage In6), the three *LOFSEP* genes become unequally redundant to promote the final meristem transition to FM (Ohmori *et al.*, 2009; Cui *et al.*, 2010; Wang *et al.*, 2010; Hu *et al.*, 2015; Wu *et al.*, 2018).

Rice *TFL1*-like genes play a conserved role in regulating inflorescence branching

TFL1-like genes in eudicots and monocots play a highly conserved role in regulating flowering time and inflorescence architecture (Shannon & Meeks-Wagner, 1991; Alvarez *et al.*, 1992;

Nakagawa *et al.*, 2002; Zhang *et al.*, 2005; Carmona *et al.*, 2007; Danilevskaya *et al.*, 2010). In Arabidopsis, loss of *TFL1* function causes early flowering and the development of determinate inflorescences with a terminal flower, compared with indeterminate WT inflorescences (Bradley *et al.*, 1997), while *TFL1* overexpression delays flowering and prevents the development of apical meristems, resulting in an increased number of flowers (Ratcliffe *et al.*, 1998; Hanzawa *et al.*, 2005).

Here, we have found that *RCN4* overexpression significantly delays flowering and causes a significant increase in the number of branches and spikelets, indicating a weakened stimulus to switch from branch meristem to SM identity (Fig. 6). The performance of our *RCN4* overexpression plants was very similar to

equivalent experiments conducted by other authors using *RCN1/2/3* (Nakagawa *et al.*, 2002; Zhang *et al.*, 2005), implying that *TFL1*-like genes in rice play a conserved role in maintaining the indeterminacy and undifferentiated state of reproductive meristems.

It is unknown how the four *RCN* genes contribute to regulate rice inflorescence architecture. *RCN1–4* were expressed in WT panicles in early inflorescence development (Fig. S9), and loss of *RCN4* did not affect panicle architecture (Fig. 4). However, of the four *RCN* genes, only *RCN4* expression responded to the loss of *OsMADS34* (Fig. S9); *RCN4* de-repression can explain the increased branching activity in *osmads34*, which is lost in *rcn4 osmads34* double mutants (Fig. 4). Thus, while *RCN* genes may have similar roles in maintaining undifferentiated meristems, they seem to have specific responses to different molecular factors, and the individual contributions of each *RCN* gene to inflorescence development are worthy of further study.

The antagonism between *LOFSEP* and *TFL*-like genes is widely conserved

We have demonstrated that *OsMADS5* and *OsMADS34* have opposing functions to *RCN4* in regulating panicle architecture: the two MADS-box genes suppress branching, while *RCN4* promotes it (Figs 2–4, 6). The ability of OsMADS5 and OsMADS34 to interact with the promoter of *RCN4*, and the dramatic de-repression of *RCN4* in *osmads34* and *osmads5 osmads34* mutants (Fig. 5), suggest that they directly target *RCN4*. A previous study in Arabidopsis has proposed that *SOC1*, *AGL24*, *SVP*, and the *LOFSEP* gene *SEP4* cooperate to suppress *TFL1* in emerging lateral meristems, thus regulating the overall inflorescence architecture, and that their orthologues in rice may play a similar role (Liu *et al.*, 2013). A similar antagonism between *OsMADS34/PAP2* orthologues and *TFL*-like genes in regulating inflorescence architecture and grain yield is also demonstrated in wheat (Wang *et al.*, 2017b) and foxtail millet (*Setaria italica*; Hussin *et al.*, 2021).

The native OsMADS5 and OsMADS34 proteins neither activated nor repressed activity of the *RCN4* upstream promoter in tobacco leaves (Fig. 5d). Either some *RCN4* regulatory sequences required for repression may have been absent (Fig. 5a,b), or the OsMADS proteins may require interaction with other proteins for full activity. Previous studies have shown the OsMADS5 and OsMADS34 have lost several conserved exon sequences and motifs in their C-terminus (Gao *et al.*, 2010; Lin *et al.*, 2014), and that OsMADS34 has lost its transcriptional activation function (Gao *et al.*, 2010; Ren *et al.*, 2016). It is also well known that SEP proteins function by forming heterotetramers with other MADS-box homeotic TFs (Goto *et al.*, 2001; Honma & Goto, 2001; Jack, 2001), and by recruiting members of different TF families and chromatin remodelling factors (Smaczniak *et al.*, 2012). Thus, OsMADS5 and OsMADS34 may depend on other TFs, chromatin regulators, and/or cofactors to properly regulate *RCN4* and other target genes, and limiting amounts or distribution of such interactors may explain the relatively mild effects of *OsMADS5* and *OsMADS34* overexpression (Fig. 3).

Implications of inflorescence architectural variations for cereal breeding

We have adopted a rigorous and detailed phenotypic approach to revisit the effect of *OsMADS34* on panicle architecture. In addition, we show that its paralogue *OsMADS5*, known only as a floral identity gene so far (Wu *et al.*, 2018), redundantly contributes to this process after the establishment of PBMs. Our results indicate that *OsMADS34* function is predominant at IM and PBM stage, while cooperating with *OsMADS5* later to suppress secondary and higher-order branching and to promote the transition from branch meristem to SM. We propose a developmental model in which *OsMADS34* specifically fine-tunes the activity of IM before its arrest, thus limiting the number of primary branches, after which *OsMADS5* and *OsMADS34* act together as potent repressors of secondary and higher-order branching, at least partially through repression of *RCN4* (Fig. 9). This second function is particularly interesting, since secondary branching has been identified as the major determinant of spikelet number and yield in rice domestication, overcoming the contribution of primary branching (Harrop *et al.*, 2019).

To be able to remodel inflorescence architecture in crops, we need to further advance our knowledge on its molecular control. Loss of rice *OsMADS5* and *OsMADS34* functions leads to strong increase in panicle branching and spikelet initiation, which is a highly desirable phenotype in breeding. However, the subsequent defects of branch abortion and elongation (Figs 2, 8; Kobayashi *et al.*, 2010) and in spikelet development (Wu *et al.*, 2018) hampers the direct use of *osmads5* and *osmads34* in breeding, similarly to *fzp* loss of function (Komatsu *et al.*, 2003; Bai *et al.*, 2016). Yet, counteracting excess branch numbers by abortion suggests the existence of compensatory mechanisms to constrain spikelet production, and deciphering this regulatory network may reveal yet unknown factors, or new functions for already identified regulators. Such new factors or alleles affecting the transcriptional or post-transcriptional regulation of *OsMADS5* and *OsMADS34* may overcome the problem of branch and spikelet abortion, similar to what has already happened with *FZP* and *SPL14* (Jiao *et al.*, 2010; Miura *et al.*, 2010; Bai *et al.*, 2017; Wang *et al.*, 2017a; Zhang *et al.*, 2017; Huang *et al.*, 2018). In addition, the various functions of *OsMADS5* and *OsMADS34* are likely to be genetically separable, as suggested by the involvement of *RCN4* exclusively in secondary and higher-order branching, but not in primary branching or rachis/branch elongation (Figs 6, 8).

Such discoveries will be assisted by the diverse transcriptomic profiles of rice IMs, branch meristems, and SMs (Harrop *et al.*, 2016) and by quantitative trait loci (QTLs) specifically affecting only primary branch formation, secondary branch/spikelet formation, and/or spikelet abortion (Yamagishi *et al.*, 2004). A recent phenotypic survey of wild and domesticated *Oryza* accessions provided more evidence that primary and secondary branch numbers are controlled by different genetic mechanisms (Harrop *et al.*, 2019), while this and previous works show that *OsMADS34* affects both (Gao *et al.*, 2010; Kobayashi *et al.*, 2010). The rate of secondary branch abortion in *osmads34* may also be influenced by environmental conditions, as suggested by
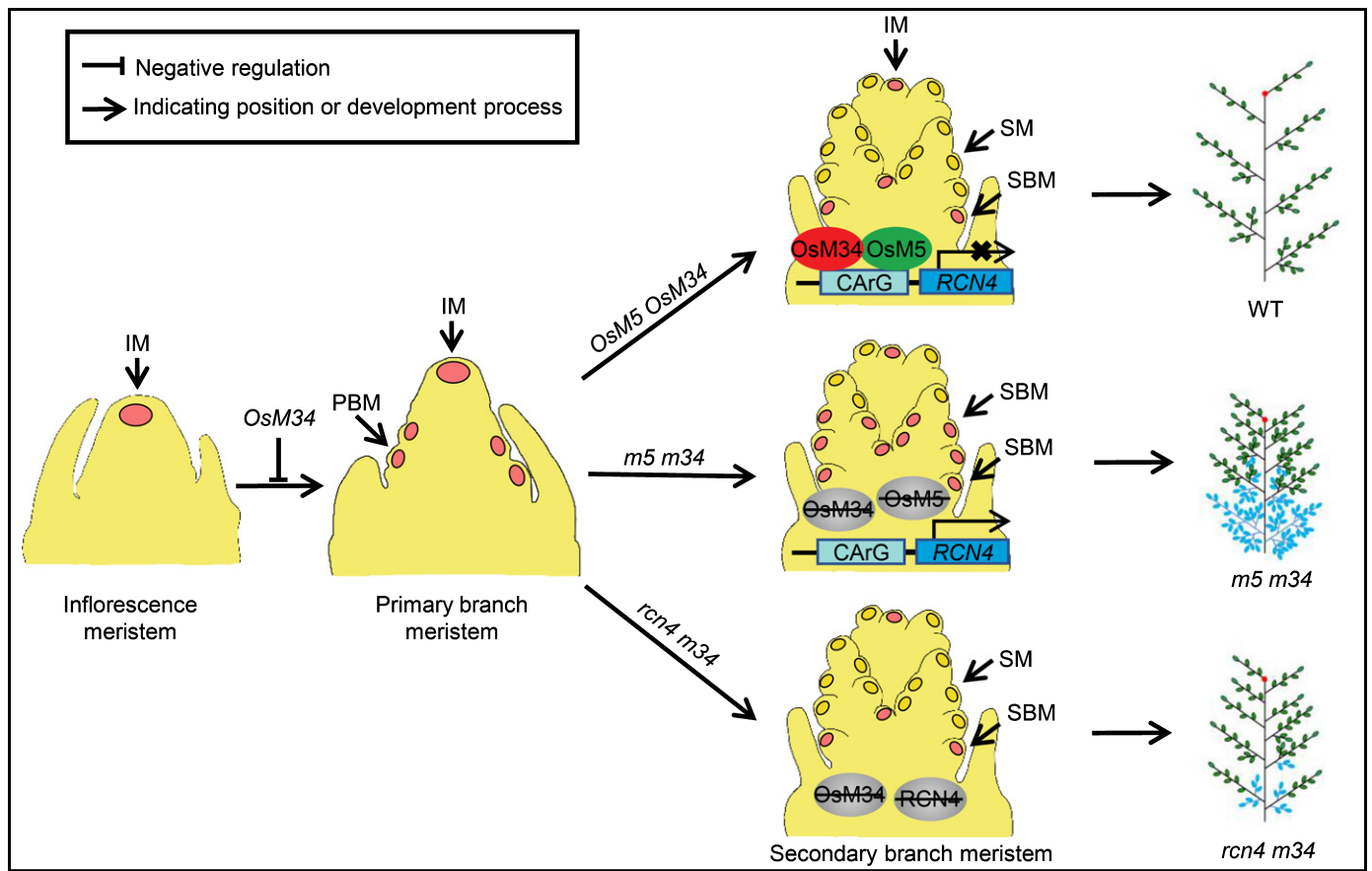
Fig. 9 Proposed model for the role of *OsMADS5* and *OsMADS34* in regulating rice inflorescence development. Inflorescence meristem (IM), primary branch meristem (PBM), and secondary branch meristem (SBM) are shown in pink. Spikelet meristems (SMs) are shown in yellow. Aborted branches and spikelets are shown in blue. *OsM5*, *OsMADS5*; *OsM34*, *OsMADS34*; WT, wild-type; *m5 m34*, *osmads5 osmads34*; *rcn4 m34*, *rcn4 osmads34*.

our preliminary phenotypic comparisons in open field in Shanghai and in the southern island of Hainan, China (W. Zhu *et al.*, unpublished), and better understanding of how these complex networks are regulated to control inflorescence development, and therefore yield, in response to physiological and environmental signal will provide new avenues to benefit molecular breeding.

Author contributions

WZ performed all the experiments. LY and XD helped collect material for qRT-PCR analysis and ChIP-qPCR assays. DW helped generate *OsMADS5* overexpression lines. QM helped generate *rcn4* mutants. LY and XC helped generate transgenic plants by *Agrobacterium*-mediated transformation. GH and JZ helped with EMSA experiments. WZ, LD, WL, CF, and DZ interpreted the results. LD, WL, and DZ designed the research and directed the project. WZ, LD, CF, and DZ wrote the manuscript with input from all authors.

ORCID

Ludovico Dreni https://orcid.org/0000-0002-2059-8420
Cristina Ferrándiz https://orcid.org/0000-0002-2460-1068
Guoqiang Huang https://orcid.org/0000-0002-6103-5704
Wanqi Liang https://orcid.org/0000-0002-9938-5793
Di Wu https://orcid.org/0000-0003-1101-1170
Liu Yang https://orcid.org/0000-0003-4402-2271

New
Phytologist

Dabing Zhang https://orcid.org/0000-0003-3181-9812
Jiao Zhang https://orcid.org/0000-0002-9106-2156
Wanwan Zhu https://orcid.org/0000-0002-3545-0090

Data availability

The data used to support the findings of this study appeared in the article and are available from the corresponding authors.

References

Agrawal GK, Abe K, Yamazaki M, Miyao A, Hirochika H. 2005. Conservation of the E-function for floral organ identity in rice revealed by the analysis of tissue culture-induced loss-of-function mutants of the *OsMADS1* gene. *Plant Molecular Biology* **59**: 125–135.

Alvarez J, Guli CL, Yu X-H, Smyth DR. 1992. terminal flower: a gene affecting inflorescence development in *Arabidopsis thaliana*. *The Plant Journal* **2**: 103–116.

Arora R, Agarwal P, Ray S, Singh AK, Singh VP, Tyagi AK, Kapoor S. 2007. MADS-box gene family in rice: genome-wide identification, organization and expression profiling during reproductive development and stress. *BMC Genomics* **8**: 242.

Bai X, Huang Y, Hu Y, Liu H, Zhang B, Smaczniak C, Hu G, Han Z, Xing Y. 2017. Duplication of an upstream silencer of *FZP* increases grain yield in rice. *Nature Plants* **3**: 885–893.

Bai X, Huang Y, Mao D, Wen M, Zhang L, Xing Y. 2016. Regulatory role of *FZP* in the determination of panicle branching and spikelet formation in rice. *Scientific Reports* **6**: 19022.

Benlloch R, Berbel A, Serrano-Mislata A, Madueno F. 2007. Floral initiation and inflorescence architecture: a comparative view. *Annals of Botany* **100**: 659–676.

Bowler C, Benvenuto G, Laflamme P, Molino D, Probst AV, Tariq M, Paszkowski J. 2004. Chromatin techniques for plant cells. *The Plant Journal* **39**: 776–789.

Bradley D, Ratcliffe O, Vincent C, Carpenter R, Coen E. 1997. Inflorescence commitment and architecture in Arabidopsis. *Science* **275**: 80–83.

Carmona MJ, Calonje M, Martínez-Zapater JM. 2007. The *FT/TFL1* gene family in grapevine. *Plant Molecular Biology* **63**: 637–650.

Chardon F, Damerval C. 2005. Phylogenomic analysis of the *PEBP* gene family in cereals. *Journal of Molecular Evolution* **61**: 579–590.

Cui R, Han J, Zhao S, Su K, Wu F, Du X, Xu Q, Chong K, Theissen G, Meng Z. 2010. Functional conservation and diversification of class E floral homeotic genes in rice (*Oryza sativa*). *The Plant Journal* **61**: 767–781.

Danilevskaya ON, Meng X, Ananiev EV. 2010. Concerted modification of flowering time and inflorescence architecture by ectopic expression of *TFL1*-like genes in maize. *Plant Physiology* **153**: 238–251.

Danilevskaya ON, Meng X, Hou Z, Ananiev EV, Simmons CR. 2008. A genomic and expression compendium of the expanded *PEBP* gene family from maize. *Plant Physiology* **146**: 250–264.

Dreni L, Jacchia S, Fornara F, Fornari M, Ouwerkerk PB, An G, Colombo L, Kater MM. 2007. The D-lineage MADS-box gene *OsMADS13* controls ovule identity in rice. *The Plant Journal* **52**: 690–699.

Fang F, Ye S, Tang J, Bennett MJ, Liang W. 2020. DWT1/DWL2 act together with OsPIP5K1 to regulate plant uniform growth in rice. *New Phytologist* **225**: 1234–1246.

de Folter S, Angenent GC. 2006. trans meets cis in MADS science. *Trends in Plant Science* **11**: 224–231.

Gao X, Liang W, Yin C, Ji S, Wang H, Su X, Guo C, Kong H, Xue H, Zhang D. 2010. The *SEPALLATA*-like gene *OsMADS34* is required for rice inflorescence and spikelet development. *Plant Physiology* **153**: 728–740.

Goto K, Kyozuka J, Bowman JL. 2001. Turning floral organs into leaves, leaves into floral organs. *Current Opinion in Plant Biology* **11**: 449–456.

Hanzawa Y, Money T, Bradley D. 2005. A single amino acid converts a repressor to an activator of flowering. *Proceedings of the National Academy of Sciences, USA* **102**: 7748–7753.

Harrop TWR, Mantegazza O, Luong AM, Béthune K, Lorieux M, Jouannic S, Adam H. 2019. A set of *AP2*-like genes is associated with inflorescence branching and architecture in domesticated rice. *Journal of Experimental Botany* **70**: 5617–5629.

Harrop TWR, Ud Din I, Gregis V, Osnato M, Jouannic S, Adam H, Kater MM. 2016. Gene expression profiling of reproductive meristem types in early rice inflorescences by laser microdissection. *The Plant Journal* **86**: 75–88.

Herr JM. 1982. An analysis of methods for permanently mounting ovules cleared in four-and-a-half type clearing fluids. *Stain Technology* **57**: 161–169.

Hiei Y, Ohta S, Komari T, Kumashiro T. 1994. Efficient transformation of rice (*Oryza sativa* L.) mediated by *Agrobacterium* and sequence analysis of the boundaries of the T-DNA. *The Plant Journal* **6**: 271–282.

Honma T, Goto K. 2001. Complexes of MADS-box proteins are sufficient to convert leaves into floral organs. *Nature* **409**: 525–529.

Hu Y, Liang W, Yin C, Yang X, Ping B, Li A, Jia R, Chen M, Luo Z, Cai Q et al. 2015. Interactions of *OsMADS1* with floral homeotic genes in rice flower development. *Molecular Plant* **8**: 1366–1384.

Huang Y, Zhao S, Fu Y, Sun H, Ma X, Tan L, Liu F, Sun X, Sun H, Gu P et al. 2018. Variation in the regulatory region of *FZP* causes increases in secondary inflorescence branching and grain yield in rice domestication. *The Plant Journal* **96**: 716–733.

Hussin SH, Wang H, Tang S, Zhi H, Tang C, Zhang W, Jia G, Diao X. 2021. SiMADS34, an E-class MADS-box transcription factor, regulates inflorescence architecture and grain yield in *Setaria italica*. *Plant Molecular Biology* **105**: 419–434.

Itoh J, Nonomura K, Ikeda K, Yamaki S, Inukai Y, Yamagishi H, Kitano H, Nagato Y. 2005. Rice plant development: from zygote to spikelet. *Plant and Cell Physiology* **46**: 23–47.

Jack T. 2001. Relearning our ABCs: new twists on an old model. *Trends in Plant Science* **6**: 310–316.

Jeon JS, Jang S, Lee S, Nam J, Kim C, Lee SH, Chung YY, Kim SR, Lee YH, Cho YG et al. 2000. leafy hull sterile1 is a homeotic mutation in a rice MADS box gene affecting rice flower development. *Plant Cell* **12**: 871–884.

Jiao Y, Wang Y, Xue D, Wang J, Yan M, Liu G, Dong G, Zeng D, Lu Z, Zhu X et al. 2010. Regulation of *OsSPL14* by OsmiR156 defines ideal plant architecture in rice. *Nature Genetics* **42**: 541–544.

Kaneko-Suzuki M, Kurihara-Ishikawa R, Okushita-Terakawa C, Kojima C, Nagano-Fujiwara M, Ohki I, Tsuji H, Shimamoto K, Taoka KI. 2018. TFL1-like proteins in rice antagonize rice FT-like protein in inflorescence development by competition for complex formation with 14-3-3 and FD. *Plant and Cell Physiology* **59**: 458–468.

Karimi M, Inzé D, Depicker A. 2002. GATEWAY vectors for *Agrobacterium*-mediated plant transformation. *Trends in Plant Science* **7**: 193–195.

Kato Y, Kamoshita A, Yamagishi J. 2008. Preflowering abortion reduces spikelet number in upland rice (L.) under water stress. *Crop Science* **48**: 2389–2395.

Kellogg EA. 2007. Floral displays: genetic control of grass inflorescences. *Current Opinion in Plant Biology* **10**: 26–31.

Khanday I, Yadav SR, Vijayraghavan U. 2013. Rice *LHS1/OsMADS1* controls floret meristem specification by coordinated regulation of transcription factors and hormone signaling pathways. *Plant Physiology* **161**: 1970–1983.

Kobayashi K, Maekawa M, Miyao A, Hirochika H, Kyozuka J. 2010. *PANICLE PHYTOMER2 (PAP2)*, encoding a *SEPALLATA* subfamily MADS-box protein, positively controls spikelet meristem identity in rice. *Plant and Cell Physiology* **51**: 47–57.

Kobayashi K, Yasuno N, Sato Y, Yoda M, Yamazaki R, Kimizu M, Yoshida H, Nagamura Y, Kyozuka J. 2012. Inflorescence meristem identity in rice is specified by overlapping functions of three *AP1/FUL*-like MADS box genes and *PAP2*, a *SEPALLATA* MADS box gene. *Plant Cell* **24**: 1848–1859.

Komatsu M, Chujo A, Nagato Y, Shimamoto K, Kyozuka J. 2003. *FRIZZY PANICLE* is required to prevent the formation of axillary meristems and to establish floral meristem identity in rice spikelets. *Development* **130**: 3841–3850.

Kyozuka J, Tokunaga H, Yoshida A. 2014. Control of grass inflorescence form by the fine-tuning of meristem phase change. *Current Opinion in Plant Biology* **17**: 110–115.

Li G, Liang W, Zhang X, Ren H, Hu J, Bennett MJ, Zhang D. 2014. Rice actin-binding protein RMD is a key link in the auxin-actin regulatory loop that

controls cell growth. *Proceedings of the National Academy of Sciences, USA* 111: 10377–10382.

Li H, Liang W, Hu Y, Zhu L, Yin C, Xu J, Dreni L, Kater MM, Zhang D. 2011. Rice *MADS6* interacts with the floral homeotic genes *SUPERWOMAN1*, *MADS3*, *MADS58*, *MADS13*, and *DROOPING LEAF* in specifying floral organ identities and meristem fate. *Plant Cell* 23: 2536–2552.

Li N, Zhang DS, Liu HS, Yin CS, Li XX, Liang WQ, Yuan Z, Xu B, Chu HW, Wang J *et al.* 2006. The rice tapetum degeneration retardation gene is required for tapetum degradation and anther development. *Plant Cell* 18: 2999–3014.

Lin X, Wu F, Du X, Shi X, Liu Y, Liu S, Hu Y, Theißen G, Meng Z. 2014. The pleiotropic *SEPALLATA*-like gene *OsMADS34* reveals that the 'empty glumes' of rice (*Oryza sativa*) spikelets are in fact rudimentary lemmas. *New Phytologist* 202: 689–702.

Liu C, Teo ZW, Bi Y, Song S, Xi W, Yang X, Yin Z, Yu H. 2013. A conserved genetic pathway determines inflorescence architecture in Arabidopsis and rice. *Developmental Cell* 24: 612–622.

Malcomber ST, Kellogg EA. 2005. *SEPALLATA* gene diversification: brave new whorls. *Trends in Plant Science* 10: 427–435.

Mao Z, He S, Xu F, Wei X, Jiang L, Liu Y, Wang W, Li T, Xu P, Du S *et al.* 2020. Photoexcited CRY1 and phyB interact directly with ARF6 and ARF8 to regulate their DNA-binding activity and auxin-induced hypocotyl elongation in Arabidopsis. *New Phytologist* 225: 848–865.

Meng Q, Li X, Zhu W, Yang L, Liang W, Dreni L, Zhang D. 2017. Regulatory network and genetic interactions established by *OsMADS34* in rice inflorescence and spikelet morphogenesis. *Journal of Integrative Plant Biology* 59: 693–707.

Miura K, Ikeda M, Matsubara A, Song XJ, Ito M, Asano K, Matsuoka M, Kitano H, Ashikari M. 2010. *OsSPL14* promotes panicle branching and higher grain productivity in rice. *Nature Genetics* 42: 545–549.

Nakagawa M, Shimamoto K, Kyozuka J. 2002. Overexpression of *RCN1* and *RCN2*, rice *TERMINAL FLOWER 1/CENTRORADIALIS* homologs, confers delay of phase transition and altered panicle morphology in rice. *The Plant Journal* 29: 743–750.

Ohmori S, Kimizu M, Sugita M, Miyao A, Hirochika H, Uchida E, Nagato Y, Yoshida H. 2009. *MOSAIC FLORAL ORGANS1*, an *AGL6*-Like MADS box gene, regulates floral organ identity and meristem fate in rice. *Plant Cell* 21: 3008–3025.

Prasad K, Parameswaran S, Vijayraghavan U. 2005. *OsMADS1*, a rice MADS-box factor, controls differentiation of specific cell types in the lemma and palea and is an early-acting regulator of inner floral organs. *The Plant Journal* 43: 915–928.

Prasad K, Sriram P, Kumar CS, Kushalappa K, Vijayraghavan U. 2001. Ectopic expression of rice *OsMADS1* reveals a role in specifying the lemma and palea, grass floral organs analogous to sepals. *Development Genes and Evolution* 211: 281–290.

Ratcliffe OJ, Amaya I, Vincent CA, Rothstein S, Carpenter R, Coen ES, Bradley DJ. 1998. A common mechanism controls the life cycle and architecture of plants. *Development* 125: 1609–1615.

Ren D, Rao Y, Leng Y, Li Z, Xu Q, Wu L, Qiu Z, Xue D, Zeng D, Hu J *et al.* 2016. Regulatory role of *OsMADS34* in the determination of glumes fate, grain yield, and quality in rice. *Frontiers in Plant Science* 7: 1853.

Shannon S, Meeks-Wagner DR. 1991. A mutation in the Arabidopsis *TFL1* gene affects inflorescence meristem development. *Plant Cell* 3: 877–892.

Smaczniak C, Immink RG, Muiño JM, Blanvillain R, Busscher M, Busscher-Lange J, Dinh QD, Liu S, Westphal AH, Boeren S *et al.* 2012. Characterization of MADS-domain transcription factor complexes in Arabidopsis flower development. *Proceedings of the National Academy of Sciences, USA* 109: 1560–1565.

Ta KN, Sabot F, Adam H, Vigouroux Y, De Mita S, Ghesquière A, Do NV, Gantet P, Jouannic S. 2016. miR2118-triggered phased siRNAs are differentially expressed during the panicle development of wild and domesticated African rice species. *Rice* 9: 10.

Tanaka W, Pautler M, Jackson D, Hirano HY. 2013. Grass meristems II: inflorescence architecture, flower development and meristem fate. *Plant and Cell Physiology* 54: 313–324.

Tao J, Liang W, An G, Zhang D. 2018. *OsMADS6* controls flower development by activating *Rice FACTOR OF DNA METHYLATION LIKE1*. *Plant Physiology* 177: 713–727.

Wang J, Yu H, Xiong G, Lu Z, Jiao Y, Meng X, Liu G, Chen X, Wang Y, Li J. 2017. Tissue-specific ubiquitination by IPA1 INTERACTING PROTEIN1 modulates IPA1 protein levels to regulate plant architecture in rice. *Plant Cell* 29: 697–707.

Wang K, Tang D, Hong L, Xu W, Huang J, Li M, Gu M, Xue Y, Cheng Z. 2010. *DEP* and *AFO* regulate reproductive habit in rice. *PLoS Genetics* 6: e1000818.

Wang Y, Yu H, Tian C, Sajjad M, Gao C, Tong Y, Wang X, Jiao Y. 2017. Transcriptome association identifies regulators of wheat spike architecture. *Plant Physiology* 175: 746–757.

Wu D, Liang W, Zhu W, Chen M, Ferrándiz C, Burton RA, Dreni L, Zhang D. 2018. Loss of LOFSEP transcription factor function converts spikelet to leaf-like structures in rice. *Plant Physiology* 176: 1646–1664.

Yamagishi J, Miyamoto N, Hirotsu S, Laza RC, Nemoto K. 2004. QTLs for branching, floret formation, and pre-flowering floret abortion of rice panicle in a temperate japonica x tropical japonica cross. *Theoretical and Applied Genetics* 109: 1555–1561.

Zahn LM, Kong H, Leebens-Mack JH, Kim S, Soltis PS, Landherr LL, Soltis DE, Depamphilis CW, Ma H. 2005. The evolution of the *SEPALLATA* subfamily of MADS-box genes: a preangiosperm origin with multiple duplications throughout angiosperm history. *Genetics* 169: 2209–2223.

Zhang D, Yuan Z. 2014. Molecular control of grass inflorescence development. *Annual Review of Plant Biology* 65: 553–578.

Zhang D, Yuan Z, An G, Dreni L, Hu J, Kater MM. 2013. Panicle development. In: Zhang Q, Wing RA, eds. *Genetics and genomics of rice*. New York, NY, USA: Springer, 279–295.

Zhang H, Zhang J, Wei P, Zhang B, Gou F, Feng Z, Mao Y, Yang L, Zhang H, Xu N *et al.* 2014. The CRISPR/Cas9 system produces specific and homozygous targeted gene editing in rice in one generation. *Plant Biotechnology Journal* 12: 797–807.

Zhang L, Yu H, Ma B, Liu G, Wang J, Wang J, Gao R, Li J, Liu J, Xu J *et al.* 2017. A natural tandem array alleviates epigenetic repression of *IPA1* and leads to superior yielding rice. *Nature Communications* 8: 14789.

Zhang S, Hu W, Wang L, Lin C, Cong B, Sun C, Luo D. 2005. *TFL1/CEN*-like genes control intercalary meristem activity and phase transition in rice. *Plant Science* 168: 1393–1408.

Supporting Information

Additional Supporting Information may be found online in the Supporting Information section at the end of the article.

Fig. S1 Mutations generated in rice *osmads5* CRISPR lines.

Fig. S2 Expression of *OsMADS5* in *c.* 1 mm rice young panicles (In6) in *osmads34* mutant and *OsMADS5* overexpression lines.

Fig. S3 Expression of *OsMADS34* in *c.* 1 mm rice young panicles (In6) in *OsMADS34* overexpression lines.

Fig. S4 Expression of *RCN4* in rice leaves of *RCN4* overexpression lines at reproductive stage.

Fig. S5 Western blot analysis of rice OsMADS34-GFP fusion protein.

Fig. S6 Complementation of the rice *osmads34-1* mutant phenotype using the *pOsMADS34::gOsMADS34-GFP* construct.

Fig. S7 Sense controls of *in situ* RNA hybridization of rice *OsMADS5* and *OsMADS34* in WT and nontransformed control for confocal imaging of the *pOsMADS34::gOsMADS34-GFP* reporter line (supports Fig. 1).

Fig. S8 Phenotypes of rice wild-type and *osmads34(I)-CRISPR* mutant panicles.

Fig. S9 Expression of rice *RCN* homologues in wild-type and *os-mads* knockout panicles at two developmental stages.

Fig. S10 Mutations generated in rice *rcn4* CRISPR lines.

Fig. S11 Bimolecular fluorescence complementation analysis of homodimerization and heterodimerization ability between rice OsMADS5 and OsMADS34 proteins in *Nicotiana benthamiana* leaves.

Fig. S12 Morphology of rice wild-type and *RCN4* overexpression plants and spikelets.

Table S1 List of primers used in this study.

Please note: Wiley Blackwell are not responsible for the content or functionality of any Supporting Information supplied by the authors. Any queries (other than missing material) should be directed to the *New Phytologist* Central Office.

About *New Phytologist*

- *New Phytologist* is an electronic (online-only) journal owned by the New Phytologist Foundation, a **not-for-profit organization** dedicated to the promotion of plant science, facilitating projects from symposia to free access for our Tansley reviews and Tansley insights.

- Regular papers, Letters, Viewpoints, Research reviews, Rapid reports and both Modelling/Theory and Methods papers are encouraged. We are committed to rapid processing, from online submission through to publication 'as ready' via *Early View* – our average time to decision is <23 days. There are **no page or colour charges** and a PDF version will be provided for each article.

- The journal is available online at Wiley Online Library. Visit **www.newphytologist.com** to search the articles and register for table of contents email alerts.

- If you have any questions, do get in touch with Central Office (np-centraloffice@lancaster.ac.uk) or, if it is more convenient, our USA Office (np-usaoffice@lancaster.ac.uk)

- For submission instructions, subscription and all the latest information visit **www.newphytologist.com**